



Thermophysical Properties of Low GWP Refrigerants: An Update

L. Fedele¹ · G. Lombardo^{1,2} · I. Greselin³ · D. Menegazzo^{1,2} · S. Bobbo¹

Received: 27 December 2022 / Accepted: 14 March 2023 / Published online: 7 April 2023
© The Author(s) 2023

Abstract

In the last decades, the industry of HVAC&R has faced continuous changes trying to identify environmentally friendly refrigerants for the numerous applications of the sector. However, the amount of low GWP fluids still available as potential refrigerants is limited to some natural fluids and, among synthetic chemicals, to hydrofluoroolefins (HFO). The knowledge of the thermophysical properties of these compounds and the evaluation of their energy efficiency in experimental apparatuses is essential to properly address the selection of the most suitable fluids. However, regarding the wide majority of HFOs, the information on the thermophysical properties, especially for the blends, are still scarce and require further research. In this work, an analysis of the possible substitutes and the available experimental data sets on their thermophysical properties was carried out to find out for which fluids further studies are needed to obtain an accurate representation of their thermophysical properties. Specifically, for 21 pure refrigerants, an overview of the thermodynamic (*critical point*, p_{sat} , *PVT*, heat capacity and speed of sound) and transport properties (λ , μ , σ) data published in the peer reviewed literature was provided. In addition, a more comprehensive analysis was carried out for four fluids (R1243zf, R1233zd(E), R1336mzz(Z), and R1224yd(Z)), for which major efforts have been made in the last 4 years to investigate the above thermophysical properties. Although an increasing amount of data sets on thermophysical properties have been compiled in recent years, the present study indicates that research efforts are still needed, especially on transport properties, as only 4 of the fluids of interest for the present research have been fully investigated (R1234yf, R1234ze(E), R1233zd(E), R1243zf), while other 4 (R1234ze(Z), R1336mzz(Z), R1224yd(Z), R1336mzz(E)) have been almost completely characterised.

Keywords Low GWP refrigerant · HFO · Thermophysical properties

Selected Papers of the 13th Asian Thermophysical Properties Conference.

✉ L. Fedele
fedele@itc.cnr.it

Extended author information available on the last page of the article

1 Introduction

In the last decades, the refrigeration industry has undergone several changes due to the need to replace the employed refrigerants with more environmentally friendly fluids. As described by Calm (2008) [1], nowadays we are facing the search of the fourth generation of refrigerants, driven by the necessity of addressing the Global Warming issues. Large restrictions have indeed been imposed to the largely used hydrofluorocarbons (HFC) by the EU F-gas Regulation (REGULATION (EU) No.517/2014) [2] due to their high GWP (Global Warming Potential), giving a big impulse to the search of environmentally benign compounds, at least as efficient and safe as the current generation. The process of high GWP refrigerants substitution, at least in Europe, has been clearly programmed by the definition of the deadlines to limit, control and eventually block the emissions of harmful refrigerants, depending on the specific HVAC&R applications [2]. In the medium-long term, all the present high GWP refrigerants should be substituted by low GWP (< 150) refrigerants, either natural (ammonia, CO₂, hydrocarbons) or synthetic. However, natural refrigerants cannot always satisfy all process requirements, due to toxicity and/or flammability issues, beside thermodynamic properties not suitable for all the applications. As refer the group of synthetic compounds, an interesting work by Mc Linden et al. (2014) [3] restricted the number of possible fluids to be used in refrigeration at a very low number of compounds. They considered a set of about 1200 candidate fluids, identified from more than 56 000 small molecules examined by applying screening criteria to be considered for GWP, flammability, stability, toxicity, and critical temperature. At the end, the number of fluids was reduced to 62. They found that no fluid is ideal in all regards: all of them have one or more negative attributes, such as poor thermodynamic properties, toxicity, chemical instability, low to moderate flammability, or very high operating pressures. Among all the considered fluids, the potential solutions were practically restricted to chemicals belonging to few groups, in particular hydro-fluoro-olefins (HFOs), hydro-chloro-fluoro-olefins (HCFOs) or hydro-fluoro-ethers (HFEs). HFOs and HCFOs are fluorinated hydrocarbons characterised by the presence of at least one carbon–carbon double bond in the molecules. The reactivity of the double bond to the atmospheric hydroxyl radical is higher than that of single bond and as a consequence the double bond compound is more unstable in atmosphere (McLinden et al., 2014 [3]); this determines a lower atmospheric lifetime and consequently a much lower GWP. However, if their double bond represents an advantage as refers to GWP and ODP, on the other hand it might pose a problem if related to their compatibility with materials, environmental safety and toxicity. Moreover, HFOs are mildly flammable and several contradictory studies on HFOs in the last years have risen some doubts on their compatibility with the environment.

To date, only few applications can employ definitive working fluids. In automotive, R1234yf has completely substituted R134a for mobile air conditioning. Few car manufacturers are now trying to produce air conditioning systems for cars basing on CO₂, but R1234yf is surely the most used. R134a has been substituted

also by R1234ze(E) for water chillers and by R600a in domestic refrigerator. For water-to-water heat pumps, R1234ze(E) can be a good alternative to R410A, while in low temperature centrifugal water chiller, R1234ze(E) can be an alternative to R123. Nevertheless, at present most of the HVAC&R applications are without proper working fluids, able to respect all the requirements given by thermodynamic and law. For stationary air conditioning, the best solution alternative to R410A has still to be found. Several alternatives have been proposed, amongst them we can consider R290, that is highly flammable, or mixtures of R32, CO₂ and R1234yf, such as R454C and R455A, where probably some optimizations of the component quantities have still to be done. Moreover, an additional problem is that these fluids are all mildly flammable. In commercial refrigeration, CO₂ is largely employed, but some applications still need to use alternatives to R134a and R404A. R290, R1234yf and R152a are interesting substitutes of R134a, but R290 is highly flammable, while R152a, still an HFC, has high GWP and can be considered only as a mid-term substitute. On the other side, R404A can be substituted by, amongst others, R290, and mixtures of R32, R1234yf and R152a, such as R457A or R454C. For heat pumps, both for residential or high temperature industrial applications, a big search is still ongoing to find the proper alternatives to R410A and R134a, and to R245fa. R245fa, used also in ORC, can be substituted by R1233zd(E) and R1234ze(Z), mildly flammable, or R1336mzz(Z), more interesting since not flammable. For ultra-low temperature applications, mixtures of R1132a and CO₂ could be possible solutions for the substitution of R23. Table 1 lists the main properties of the working fluids, pure compounds and mixtures, considered as potential substitutes to hydrocarbons for the abovementioned applications.

It is a fact that for several applications, pure compounds, natural or synthetic, are not enough and mixtures are necessary. Mixing different fluids, it is possible to shape the final properties of the refrigerant, in terms of thermodynamic properties, but also of GWP or flammability. However, mixtures can present a high temperature glide, that is an important drawback for HVAC&R applications. In many cases, the use of new refrigerants involves the redesign of some system components, such as the compressor, the heat exchanger, or the expansion device. Moreover, in most cases, the new refrigerants can be flammable, especially in the case of hydrocarbons, or mildly flammable, as for HFOs, and this aspect requires specific measures. At last, but not least, we need to consider finding the optimal compromise between coefficient of performance (COP) and volumetric heating capacity (VHC).

Considering all the premises, thermodynamic analysis, energy balance and components design require the knowledge of the refrigerants behaviour in terms of thermodynamic and thermophysical properties such as critical parameters, vapour pressure, PvT properties, specific heat capacity, speed of sound, thermal conductivity, viscosity and surface tension, which are necessary to understand the behaviour of the fluid and to develop proper and dedicated equations of state and transport properties models that can work as a reference to calculate the refrigerant properties and design the entire system. Few years ago, Bobbo et al. (2018) performed a wide literature analysis to evaluate the amount of data available in the open literature for the most promising fluids belonging to these groups. At that time, it emerged that only

Table 1 Potential substitutes to the largely used working fluids for different applications

Application	Fluid	GWP	ASHRAE Safety Class	<i>NBP</i> (°C)	Composition (wt.%)
MTHPs, Commercial refrigeration	R134a	1330	A1	247.08	–
	R290	0.02	A3	231.01	–
	R1234yf	1 <	A2L	243.66	–
	R1234ze(E)	6	A2L	254.18	–
	R513A	573	A1	243.55	R134a/R1234yf (44/56)
	R515B	299	A1	254.15	R1234ze(E)/R227ea (91.1/8.9)
	R516A	131	A2L	243.55	R134a/R1234yf/R152a (8.5/77.5/14)
	R450A	547	A1	249.55	R134a/R1234ze(E) (42/58)
	R245fa	858	B1	288.2	–
	R1233zd(E)	3.88	A1	291.41	–
HTHPs	R1234ze(Z)	1.4	A2L	282.88	–
	R1336mzz(Z)	2	A1	306.6	–
	R1224yd(Z)	2.08	A1	287.77	–
	R23	18.4	A1	191.13	–
	R1132a	0.05	A2	190.15	–
Low temperature	CO ₂	1	A1	216.59 (triple point)	–
	R410A	1924	A1	222.55	R32/R125 (50/50)
AC, MTHPs	R290	0.02	A3	231.01	–
	R32	677	A2L	221.45	–
	R454B	466	A2L	222.45	R32/R1234yf (68.9/31.1)
	R452B	675	A2L	227.25	R32/R125/R1234yf (67/7/26)
	R447A	572	A2L	223.85	R32/R125/R1234ze(E) (68/3.5/28.5)
	R454C	166	A2L	227.35	R32/1234yf (21.5/78.5)
	R-455A	148	A2L	221.15	R744/32/1234yf (3.0/21.5/75.5)

Table 1 (continued)

Application	Fluid	GWP	ASHRAE Safety Class	NBP (°C)	Composition (wt.%)
Commercial refrigeration	R404A	3943	A1	226.93	R125/143a/134a (44/52/4)
	R290	0.02	A3	231.01	–
	R457A	159	A2L	230.57	R32/1234yf/152a (18/70/12)
	R454C	166	A2L	227.35	R32/1234yf (21.5/78.5)
	R-455A	148	A2L	221.15	R744/32/1234yf (3.0/21.5/75.5)
	R-448A	1387	A1	226.85	R32/125/1234yf/134a/1234ze(E) (26/26/20/21/7)
	R-449A	1397	A1	227.25	R32/125/1234yf/134a (24.3/24.7/25.3/25.7)

Bold indicates the fluids which need to be substituted

two fluids, out of the 17 analysed, were already well studied, namely R1234yf and R1234ze(E). Other two fluids (R1234ze(Z) and R1233zd(E)) had at least one set of data available for all except one of the seven thermophysical properties considered in the analysis. For all the other fluids, only few sets of data or no data at all were found. In this paper, the situation will be updated by analysing the open literature in the period 2018 to 2022, to identify the new sets of experimental data produced for the main thermophysical properties regarding potentially alternative synthetic low GWP refrigerants. After a description of the methodology applied, the sets of data found for each fluid will be synthesised in tables and briefly discussed.

2 Literature Analysis for the Period 2018 to 2022

2.1 Available Experimental Data

A thorough analysis of the open literature was conducted in a previous review paper by Bobbo et al. 2018 [4], which listed experimental data on the key thermodynamic (critical point, saturation pressure, PVT properties, speed of sound) and transport (thermal conductivity, viscosity and surface tension) properties of fluids considered as potential working fluids for HVAC&R applications. Fluids characterised by low global warming potential (< 150) and belonging to the groups of hydrofluoroolefins (HFO), hydrochlorofluoroolefins (HCFO) or hydrofluoroethers (HFE) were considered. The review revealed that only for 2 fluids (i.e., R1234yf, R1234ze(E)) at least one set of experimental data was available for each of the main thermophysical properties considered in the analysis, while for the other 2 fluids (R1234ze(Z) and R1233zd(E)) no data sets were available for only one property (isobaric heat capacity and thermal conductivity, respectively). Here, the available literature data for all fluids included in the Bobbo et al. study are updated with the data sets reported in the literature since 2018. In addition, this study also considers four new fluids to be used for HVAC&R and ORC applications that were recently added to ANSI / ASHRAE Standard 34 (R1224yd(Z), R131I, R1132a, R1130(E)), along with HFE RE356mmz, which is suitable for organic Rankine cycle and high temperature heat pump applications. The ASHRAE designations, IUPAC names and basic properties of the HFOs, HCFOs and HFEs considered in this article are listed in Table 2.

In particular, this paper provides a more in-depth analysis for those fluids that meet the following three criteria:

- (1) Fluids for which at least 7 of the 8 thermophysical properties considered in this study have been experimentally investigated in at least one available data set: as shown in Table 3, which lists the number of papers providing experimental data for each refrigerant, only 8 fluids are fully or almost fully characterised (i.e., R1234yf, R1243zf, R1234ze(E), R1234ze(Z), R1233zd(E), R1336mzz(E), R1336mzz(Z), R1224yd(Z)), with at least 1 data set available for each thermophysical property, except for R1234ze(Z), R1336mzz(Z), and R1224yd(Z), for which specific heat capacity data are still missing).

Table 2 ASHRAE designation, IUPAC name, and selected properties of several working fluids (data are taken from [5], unless noted otherwise)

ASHRAE designation	IUPAC name	MM (kg/kmol)	T _b (K)	T _{crit} (K)	P _{crit} (kPa)	ω	GWP ₁₀₀
R1132a ^c	1,1-Difluoroethene	64	190.15	303.6	4461.0 ^f	0.181 ^f	0.05
R1141	Fluoroethene (vinylfluoride)	46.04	N.A	N.A	N.A	N.A	1 ^b
R1123	1,1,2-Trifluoroethene	82.03	214.06	331.73	4542.6	0.261	3 ^b
R1132(E)	<i>Trans</i> -1,2-difluoroethene	N.A	N.A	350.1 ^a	6770.0 ^a	N.A	1 ^b
R1234yf	2,3,3,3-Tetrafluoropropene	114.04	243.7	367.85	3382.2	0.276	<1 ^b
R1243zf	3,3,3-Trifluoroprop-1-ene	96.05	247.73	376.93	3517.9	0.2604	0.8 ^a
R131I	Trifluoriodomethane	195.91	251.29	396.44	3953	0.176	1 ^c
R1234ye(E) ^g	<i>Trans</i> -1,2,3,3-tetrafluoroprop-1-ene	N.A	251.15	391.7 ^a	4450 ^a	0.290	2.3 ^a
R1234ze (E)	<i>Trans</i> -1,3,3,3-tetrafluoropropene	114.04	254.18	382.51	3634.9	0.313	6 ^a
R1225ye(Z) ^g	<i>Cis</i> -1,2,3,3,3-pentafluoroprop-1-ene	132.03	253.62	380.05	3529	0.326	2.9 ^a
R1132(Z)	<i>Cis</i> -1,2-difluoroethene	N.A	N.A	365.1 ^a	5320 ^a	N.A	1 ^b
R1225ye(E) ^g	<i>Trans</i> -1,2,3,3,3-pentafluoroprop-1-ene	132.03	258.15	353.8 ^a	3740 ^a	0.313	2.9 ^a
R1336mzz(E) ^g	<i>Trans</i> -1,1,1,4,4,4-hexafluoro-2-butene	164.1	280.55	410.85	3533.0 ^e	0.327 ^e	17.9 ^c
R1234ze(Z)	<i>Cis</i> -1,3,3,3-tetrafluoroprop-1-ene	114.04	282.88	423.27	3530.6	0.3274	1.4 ^a
R1224yd(Z)	<i>Cis</i> -1-chloro-2,3,3,3 tetrafluoropropene	148.49	287.77	428.69	3337	0.322	2.08 ^c
R1354mzy(E)	<i>Trans</i> -1,1,1,3-tetrafluoro-2-butene	128.07	289 to 291	N.A	N.A	N.A	N.A
R1233zd(E)	<i>Trans</i> -1-chloro-3,3,3-trifluoro-1-propene	130.5	291.41	439.6	3623.7	0.3025	3.88 ^c
R1354myf(E)	<i>Trans</i> -2,4,4,4-tetrafluoro-2-butene	128.07	N.A	N.A	N.A	N.A	N.A
R1336mzz(Z)	<i>Cis</i> -1,1,1,4,4,4-hexafluoro-2-butene	164.06	306.6	444.5	2903	0.386	2 ^d

Table 2 (continued)

ASHRAE designation	IUPAC name	MM (kg/kmol)	T_b (K)	T_{crit} (K)	P_{crit} (kPa)	ω	GWP ₁₀₀
R1130(E) ^c	<i>trans</i> -1,2-dichloroethene	96.9	320.85	507.25	5510.0 ^d	0.2137 ^f	5
RE356mmz ^h	1,1,1,3,3,3-Hexafluoro-2-methoxypropane	182.06	323.99	459.58	2699	N.A	2

^aMcLinden et al. 2014 [3]^bMcLinden et al. 2015 [6]^cGimenez-Prades 2022 [7]^dMyhre et al. 2014 [8]^eTanaka et al. 2017 [9]^fomassetti et al. 2021 [10]^gBrown et al. 2010 [11]^hAlam et al. 2019 [12]ⁱTanaka 2022 [13]^lFedele et al. 2016 [14]

Table 3 Number of peer-reviewed literature references reporting experimental data/estimations for important thermophysical properties of several HFO and HCFO refrigerants (the same paper can report sets of data for different properties)

ASHRAE designation	Thermodynamic Properties					Transport Properties		
	<i>CP</i>	<i>P_{sat}</i>	<i>PVT</i>	<i>c⁰, c_p, c_v</i>	<i>w</i>	<i>σ</i>	<i>μ/ν</i>	<i>λ</i>
R1132a	1	1	1	1				
R1141								
R1123	2	3	5		1	2		
R1132(E)	1	1	1					
R1234yf	2	12	12	9	4	3	7	1
R1243zf	2	5	3	2	1	2	1	1
R131I	2	2	4	1	1	1		
R1234ye(E)								
R1234ze (E)	2	13	15	8	4	3	4	3
R1225ye(Z)		1	1					
R1132(Z)								
R1225ye(E)								
R1336mzz(E)	2	2	2		1	1	3	2
R1234ze(Z)	2	9	7		3	1	3	1
R1224yd(Z)	2	3	3		1	2	2	1
R1354mzy(E)	1	1	3					
R1233zd(E)	2	8	7	2	5	4	5	2
R1354myf(E)			1					
R1336mzz(Z)	1	4	3		2	1	3	2
R1130(E)		2	1			1		
RE356mmz	1	1	3	1	1		1	1

- (2) Fluids for which a fundamental equation of state (FES), explicit in Helmholtz energy, is implemented in the open-source software REFPROP 10.0 [5]. Equations of state are necessary to calculate the properties of the working fluids in an HVAC&R system: without them, the achievement of an optimal system design is far-fetched. In the following, the reference values for thermodynamic properties are calculated using REFPROP 10.0 and thus for each fluid the respective EoS available in the software is applied. Table 4 lists the fundamental equations of state already implemented in REFPROP 10.0. As can be seen in the Table, only 9 of the 27 fluids considered in this study have an EoS already included in the latest version of the software (i.e., R1234yf, R1234ze(E), R1233zd(E), R1243zf, R1234ze(Z), R1336mzz(Z), R1224yd(Z), R131I and R1123).
- (3) Fluids for which a larger number of available data sets were found from 2018 to 2022: Fig. 1 shows, for each thermophysical property, the number of peer-reviewed references available in 2018 (Bobbo et al. [4]) and in 2022, displaying only the six fluids that can be considered fully characterised (point 1) and for which an EoS is already implemented in REFPROP 10.0 (point 2) (R1234yf,

Table 4 Helmholtz form EoS for the considered fluids

ASHRAE designation		References	EoS uncertainties		PVT properties		w	
			P_{sat}					
R1132a	Low (2018) [15]		up to 1.07 %	(RMSD)	Compressed liquid and supercritical	0.61 % (RMSD)	1.16 % (RMSD)	n.d.
R1123	Akasaka et al. (2016) [16]	Vapor and gas phase				0.89 % (RMSD)		
		Saturated vapor and liquid				1.12 % (RMSD)		
		Vapor	0.1 %		1 %			Vapor 0.2 %
		Liquid	Higher for temperatures below 300 K	0.2 %				
R1234yf	Akasaka et al. (2020) [17]	Critical region				up to 2 %		
		Vapor	0.1 %			0.20 %	1 %	Vapor 0.03 %
		Liquid				0.10 %		
		Critical region				Up to 1.5 %		
R1234yf	Akasaka (2011) [18]	Liquid	0.1 %			0.10 %	2 %	Vapor 0.05 %
		Vapor				0.30 %		
		T 240 K to 320 K, P up to 10 MPa	0.1 %			0.10 %	5 %	Vapor 0.10 %
		Outside of this region and in the vapor phase				up to 0.5 %		Liquid 0.50 %
R1123	Rykov et al. (2019) [20]	Critical region				> 0.5 %		
		$230 \leq T \leq 420$ K	n.d			up to 0.22 % (RMS)	0.46 % (RMS)	Up to 0.88 % (RMS)
		$0.001 < p < 20$ MPa						
R1123	Lemmon and Akasaka (2022) [21]	Vapor	0.1 % (above 270 K)			0.20 %	1 % (vap. c_p)	Vapor 0.02 %
		Liquid above 40 MPa	0.3 % (lower T)			0.10 %	2 % (liq. c_p)	Liquid 0.05 %
		Liquid below 40 MPa				0.25 %	2 % (liq. c_p)	

Table 4 (continued)

ASHRAE designation		References	EoS uncertainties	PVT properties			w
			P_{sat}		c_p	c_p	c_v
R1243zf	Akasaka et al. (2016) [22]	0.1 %	Vapor	0.6 %	n.d	Vapor	n.d
			Liquid	0.05 %	n.d	Liquid	n.d
	Akasaka and Lemmon (2019) [23]	0.1 %	Vapor	0.6 %	n.d		n.d
			Liquid	0.05 %	n.d		n.d
			Critical region	Up to 1 %			
R131I	Lemmon and Span (2015) [24]	0.1 %	Vapor	0.30 %	n.d	Vapor	0.10 %
			Liquid	0.10 %	n.d	Liquid	n.d
R1234ze (E)	Akasaka (2011) [18]	0.1 %	Liquid	0.10 %	3 %	Vapor	0.05 %
			Vapor	0.20 %			
	Thol and Lemmon (2016) [25]	0.1 %	T 200 K to 380 K	0.10 %	5 %	Vapor	0.05 %
			P up to 40 MPa				
			Outside of this region and in the vapor phase	Up to 0.5 %	n.d.	Liquid	0.20 %
			Critical region	> 0.5 %			
	Astina et al. (2021) [26]	0.1 % (AAD)	Vapor	0.39 % (AAD)	1.5 % (AAD)	Vapor	0.06 % (AAD)
			Liquid	0.08 % (AAD)		Liquid	0.12 % (AAD)
			Saturated Vapor	1 % (AAD)			
			Saturated Liquid	0.11 % (AAD)			

Table 4 (continued)

ASHRAE designation	References	EoS uncertainties	PVT properties	c_p , c_p , c_v	w
		P_{sat}			
R1336mzz(E)	Akasaka et al. (2022) [27]	0.1 %	Vapor Liquid Saturated Vapor Saturated Liquid	n.d.	Vapor 0.05 % Liquid n.d.
R1234ze(Z)	Akasaka et al. (2014) [28] Akasaka and Lemmon (2019) [23]	0.15 % 0.1 % (above 300 K) 0.3 % (lower T)	Critical region Vapor Liquid Vapor Liquid	n.d. n.d. n.d. n.d.	Vapor 0.05 % Vapor Liq- uid
R1224yd(Z)	Akasaka et al. (2017) [29]	0.05 %	Critical region Liquid Saturated liquid	n.d. n.d.	Vapor 0.03 %
R1233zd(E)	Mondejar et al. (2015) [30]	0.22 % (RMS)	Critical region	n.d.	0.13 % (RMS)
R1336mzz(Z)	Akasaka and Lemmon (2022) [31] McLinden and Akasaka (2020) [32]	0.07 % (above 291 K) 0.2 % (lower T) 0.05 %	Vapor Liquid Saturated liquid Vapor Liquid	n.d. n.d. n.d. n.d. n.d.	Vapor 0.08 % Liquid 0.05 % Vapor 0.05 % Liq- uid

Reference EoS implemented in REFPROP 10.0 and used to calculate the reference values for the thermodynamic properties are shown in bold type

R1243zf, R1234ze(E), R1234ze(Z), R1233zd(E), R1336mzz(Z); R1224yd(Z) is not considered as it was not included in the previous review by Bobbo et al.). As can be seen from the figure, the 3 fluids R1243zf, R1233zd(E) and R1336mzz(Z) displayed a higher percentage increase in the number of published articles for all the considered properties, thus demonstrating a growing interest in these fluids from the scientific community; for this reason, particular attention is paid in this article towards R1243zf, R1233zd(E) and R1336mzz(Z), plus the fourth refrigerant R1224yd(Z), which was not included in the previous study (Bobbo et al., 2018 [4]).

For these four fluids, selected as described above, the following text proposes an extended analysis only for newly published articles (2018 to 2022) and for articles published before 2018 and not included in the review by Bobbo et al. [4]. On the other hand, in the following figures and tables, all data sets available so far for each of the above-mentioned refrigerants are listed, unless otherwise stated.

2.2 Thermodynamic Properties

2.2.1 Critical Point

Experimental data for the critical parameters are available for 14 of the selected refrigerants reported in Table 2; values for critical temperature T_c , critical density ρ_c , and critical pressure p_c are listed in Table 5 and graphically displayed in Fig. 2a and b as they are distributed in the P - T and ρ - T planes. For all the reported data sets critical temperatures and densities were directly measured, while the critical pressure p_c is usually either extrapolated from T_c or calculated as an adjustable parameter during vapor pressure curve regression, as indicated in Table 5.

2.2.2 Vapor Pressure

Experimental vapour pressure data are available for 16 of the selected refrigerants and for each fluid they are listed in Table 6 together with the respective deviations from REFPROP 10.0 [5].

R1243zf: 5 datasets with a total of 185 data points were identified in the peer-reviewed literature, three of which were published after the 2018 review: Higashi et al. (2018) [39] reported 20 data measured in the temperature range $T_r=0.82$ to 0.99. They show excellent agreement with REFPROP 10.0 with almost all positive deviations (AAD%=0.03 % and a maximum absolute deviation MAD % = 0.065 %). Yang et al. (2019) [53] presented 17 data points distributed over a medium range of temperature $T_r=0.72$ to 0.94. The deviations are AAD%=0.15 % and a MAD%=0.50 %, with fluctuations between positive and negative deviations, higher at the lower temperatures. Finally, Yin et al. (2020) [54] provided 26 data points in a wide range of $T_r=0.67$ to 0.99, with unbiased deviations over the whole temperature range and AAD%=0.11 %, MAD%=0.18 %. Results for this fluid are shown in Fig. 3a.

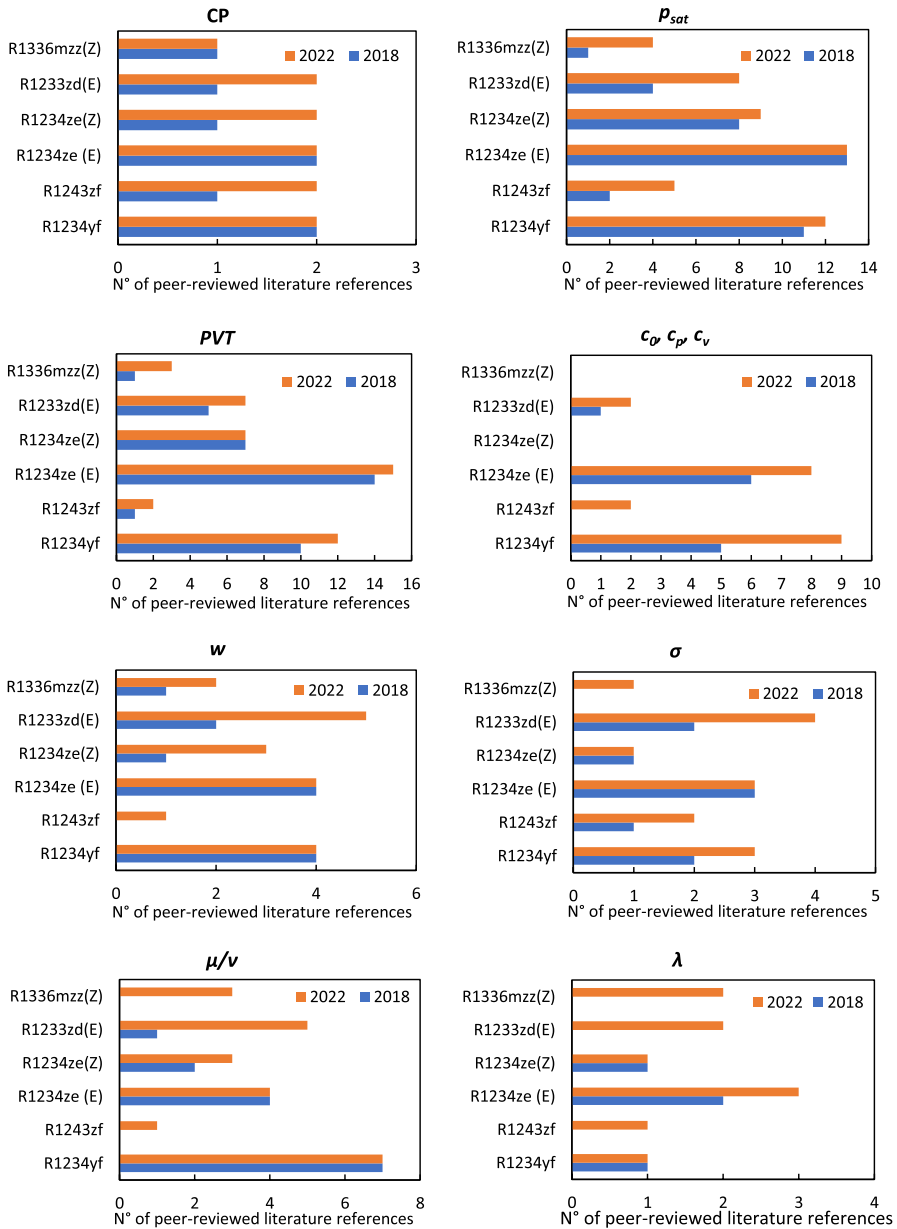


Fig. 1 Number of peer-reviewed literature references available in 2018 and 2022 for each considered thermophysical property

R1224yd(Z): 3 data sets with a total of 112 data points were identified in the literature. Sakoda and Higashi (2019) [47] present 15 data in the range $T_r=0.72$ to 0.96 with systematic negative deviations from REFPROP (AAD%=0.35 %, ,

Table 5 Available experimental data for the critical parameters of the selected fluids

ASHRAE designation	References	T_{crit} (K)	P_{crit} (MPa)	ρ_{crit} ($\text{kg}\cdot\text{m}^{-3}$)
R1132a	Low (2018) [15]	302.81	4.461	–
R1123	Fukushima et al. (2015) [33]	331.80	4.545 ^a	510
	Higashi and Akasaka (2016) [34]	332.73	4.546 ^a	504
R1132(E)	Sakoda et al. (2022) [35]	348.82	–	438
R1234yf	Tanaka and Higashi (2010a) [36]	367.85	3.382 ^a	478
	Hulse et al. (2009) [37]	367.95	3.260 ^a	–
R1243zf	Daubert et al. (1987) [38]	378.55	3.609	–
	Higashi and Sakoda (2018) [39]	376.93	3.518 ^a	414
R1311	Duan et al. (1999) [40]	396.44	3.953 ^a	868
	Perera et al. (2022) [41]	396.49	3.971	865
R1234ze(E)	Higashi and Tanaka (2010) [42]	382.51	3.632 ^a	486
	Grebenkov et al. (2009) [43]	382.75	3.681 ^a	–
R1336mzz(E)	Tanaka et al. (2017a) [9]	403.37	2.766	515
	Sakoda et al. (2021) [44]	403.50	2.779	513
R1234ze(Z)	Higashi et al. (2015) [45]	423.27	3.533 ^b	470
	Tanaka et al. (2020) [46]	423.34	3.521	459
R1224yd(Z)	Sakoda and Higashi (2019) [47]	428.69	3.331 ^b	535
	Tanaka et al. (2021) [48]	428.82	3.327	541
R1354mzy(E)	Kimura et al. (2017a) [49]	424.73	3.250	424
R1233zd(E)	Hulse et al. (2012a) [50]	438.86	3.772 ^a	–
	Tanaka et al. (2021) [48]	438.86	3.558	487
R1336mzz(Z)	Tanaka et al. (2017b) [51]	444.50	2.895	507
RE356mmz	Sako et al. (1998) [52]	459.58	2.699	481

^aExtrapolated to T_{crit}

^bTreated as an adjustable parameter during vapor pressure curve regression

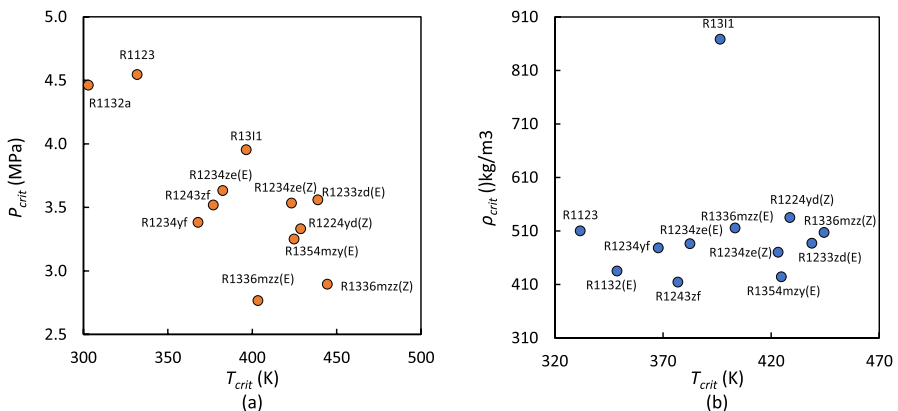


Fig. 2 Critical parameters obtained from experimental measurements. (a) Critical pressure as a function of critical temperature; (b) critical density as a function of critical temperature

Table 6 Available experimental data for the vapour pressure of selected refrigerants

ASHRAE designation	Reference	No. data	T range (K)	AAD%
R1132a	Tomassetti et al. (2021) [10]	24	223 ÷ 281	–
R1123	Fukushima et al. (2015) [33]	16	313 ÷ 331	0.58
	Higashi and Akasaka (2016) [34]	13	300 ÷ 331	0.03
	Higashi et al. (2018) [61]	27	278 ÷ 332	0.09
R1132(E)	Perera et al. (2022) [62]	24	240 ÷ 349 (T_c)	0.02
R1234yf	Chen et al. (2015a, 2015b) [63]	5	293 ÷ 323	0.05
	Di Nicola et al. (2010b) [64]	34	224 ÷ 366	0.14
	Fedele et al. (2011) [65]	40	246 ÷ 343	0.07
	Hu et al. (2017b) [66]	9	283 ÷ 323	0.11
	Hulse et al. (2009) [37]	12	241 ÷ 353	1.36
	Kamiaka et al. (2013) [67]	7	273 ÷ 333	0.17
	Kochenburger et al. (2017) [68]	5	193 ÷ 273	0.24
	Madani et al. (2016) [69]	7	254 ÷ 348	0.15
	Richter et al. (2011) [19]	28	250 ÷ 320	0.05
	Tanaka and Higashi (2010a) [36]	11	310 ÷ 360	0.12
	Yang et al. (2016a) [70]	4	283 ÷ 313	0.03
	Yin et al. (2019) [71]	24	253 ÷ 367	0.02
R1243zf	Brown et al. (2013) [72]	83	234 ÷ 373	0.16
	Daubert et al. (1987) [38]	39	256 ÷ 379	–
	Higashi et al. (2018) [39]	20	310 ÷ 377	0.03
	Yang et al. (2019) [53]	17	273 ÷ 353	0.15
	Yin et al. (2020) [54]	26	253 ÷ 376	0.11
R131I	Duan et al. (1996) [73]	60	243 ÷ 393	0.04
	Perera et al. (2022) [41]	37	238.9 to T_c	0.55
R1234ze(E)	Di Nicola et al. (2012a) (CNR-ITC) [74]	49	259 ÷ 343	0.1
	Di Nicola et al. (2012a) (UnivPM) [74]	29	223 ÷ 348	0.22
	Dong et al. (2011) [75]	4	258 ÷ 283	0.56
	Dong et al. (2012) [76]	4	258 ÷ 288	0.52
	Dong et al. (2013) [77]	4	258 ÷ 288	0.06
	Gong et al. (2016a) [78]	10	253 ÷ 293	0.33
	Grebenkov et al. (2009) [43]	49	237 ÷ 379	1.94
	Hu et al. (2017c) [79]	9	283 ÷ 323	0.11
	Kayukawa and Fuji (2009) [80]	32	258 ÷ 330	0.71
	McLinden et al. (2010) [81]	28	261 ÷ 280	0.03
	Tanaka (2016a) [82]	18	300 ÷ 380	0.04
	Tanaka et al. (2010a) [83]	8	310 ÷ 380	0.03
	Yin et al. (2018) [84]	15	303 ÷ 373	0.05
R1225ye(Z)	Fedele et al. (2016) (2 labs) [14]	96	233 ÷ 366	–
R1336mzz(E)	Tanaka et al. (2017a) [9]	17	323 ÷ 403	–
	Sakoda et al. (2021) [44]	26	287 ÷ 403	–
R1234ze(Z)	Fedele et al. (2014a) (CNR-ITC) [85]	28	238 ÷ 373	0.6
	Fedele et al. (2014a) (UnivPM) [85]	5	253 ÷ 293	0.22

Table 6 (continued)

ASHRAE designation	Reference	No. data	T range (K)	AAD%
	Gong et al. (2016b) [78]	19	310÷420	0.11
	Higashi et al. (2015) [45]	49	273÷373	N.A
	Kayukawa et al. (2012) [86]	4	353÷413	0.1
	Sakoda et al. (2017) [87]	22	300÷400	0.32
	Tanaka (2016a) [82]	63	273÷373	0.51
	Zhuo et al. (2017) [88]	25	290÷373	0.17
	Zhang et al. (2019) [89]	31	293÷353	0.42
R1224yd(Z)	Bobbo et al. (2020) [55]	15	310÷410	0.35
	Sakoda and Higashi (2019) [47]	66	274÷338	0.45
	Beltramino et al. (2022) [56]	14	340÷410	–
R1354mzy(E)	Kimura et al. (2017b) [90]	32	293÷353	0.33
R1233zd(E)	Di Nicola et al. (2017) (CNR-ITC) [91]	49	234÷375	0.59
	Di Nicola et al. (2017) (UnivPM) [91]	16	263÷353	1.93
	Hulse et al. (2012) [50]	95	253÷431	0.15
	Li et al. (2019) [57]	12	300÷410	0.21
	Sakoda et al. (2020) [58]	18	288÷373	0.12
	Yin et al. (2021) [59]	11	300÷400	0.29
	Tanaka et al. (2016) [92]	23	280÷438	0.09
	Mondejar et al. (2015) [30]	13	324÷443	0.15
R1336mzz(Z)	Tanaka et al. (2016) [82]	18	293÷440	0.03
	McLinden and Akasaka (2020) [32]	17	290÷410	0.18
	Sakoda et al. (2020) [58]	91	278÷443	0.23
	Li et al. (2020) [60]	12	273÷320	–
R1130(E)	Machat et al. (1985) [93]	12	273÷320	–
	Tanaka et al. (2022) [13]	14	324÷454	–

AAD relative to the EOS cited in Table 4

MAD%=0.53 %). Bobbo et al. (2020) [55] measured 31 vapour pressures in the limited temperature range $T_r=0.68$ to 0.82; the deviations are systematically positive, with AAD%=0.42 % and MAD%=0.79 %. More recently, Beltramino et al. (2022) [56] performed two measurement runs in the temperature range from 274 K to 338 K, consisting of a total of 66 data points in a reduced range ($T_r=0.64$ to 0.79); for both runs, the deviations are consistently negative, with a global AAD% of 0.45 % and a maximum deviation MAD%=0.63 %. Results for R1224yd(Z) are shown in Fig. 3b.

R1233zd(E): a total of 256 vapour pressure points and 8 data sets were published for this fluid, 4 of which were not included in the previous review: Tanaka et al. (2017) [51] measured 11 vapour pressures in the temperature range $T_r=0.68$ to 0.91, showing systematic negative deviations from REFPROP 10.0 with higher values at lower temperatures (AAD%=0.12 %, MAD%=0.15 %). The data of Li et al. (2019) [57] cover a wide temperature range ($T_r=0.58$ to 0.98) and vary

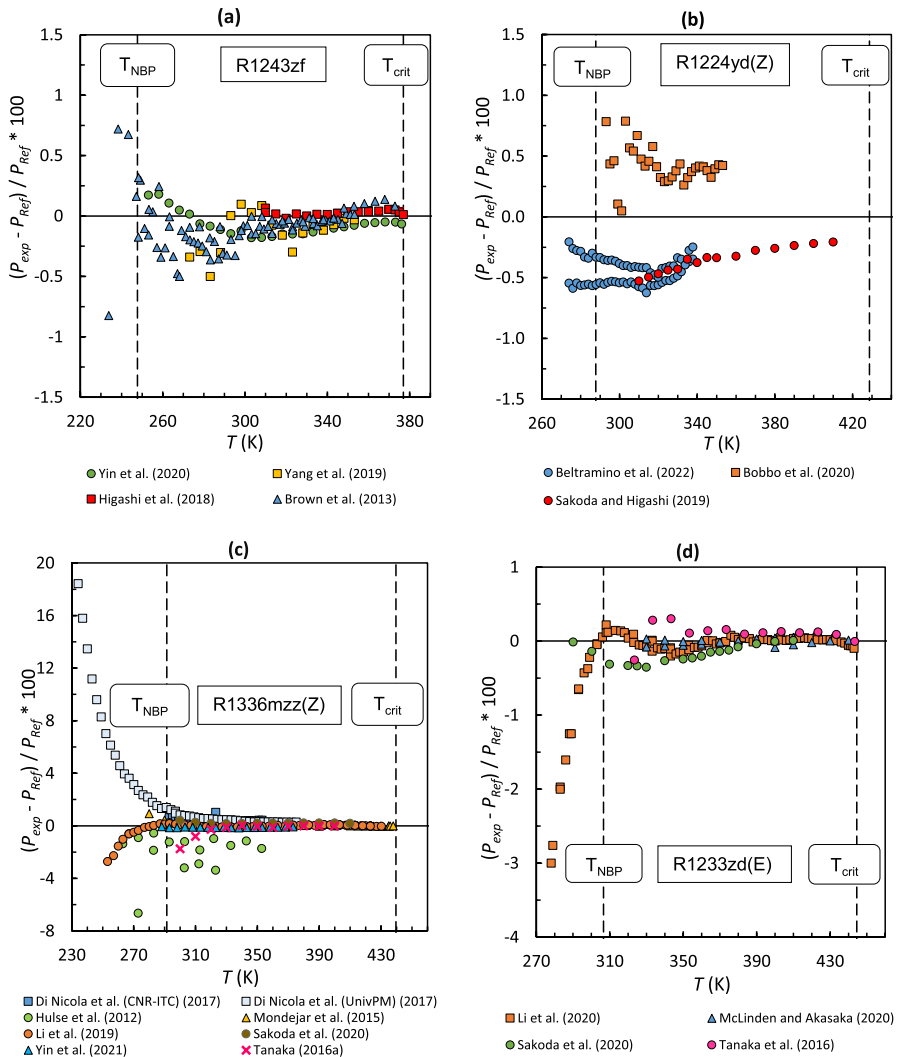


Fig. 3 Deviations of the experimental vapor pressure data for (a) R1243zf, (b) R1224yd(Z), (c) R1233zd(E) and (d) R1336mzz(Z) from the values calculated using REFPROP 10.0

between positive and negative deviations. They show $AAD\% = 0.15\%$, but a definite high maximum deviation of $MAD\% = 2.73\%$ due to increasing deviations for temperatures below 273.15 K (up to a maximum of 2.73% at 253.17 K). Sakoda et al. (2020) [58] present 12 data from $T_r = 0.68$ to $T_r = 0.93$ with systematic positive deviations from REFPROP 10.0 ($AAD\% = 0.21\%$, $MAD\% = 0.41\%$). A small amount of data is also presented by Yin et al. (2021) [59], with 18 vapour pressure data points over a medium temperature range $T_r = 0.66$ to 0.85 with systematic negative deviations $AAD\% = 0.12\%$ and $MAD\% = 0.15\%$. Results for R1233zd(E) are shown in Fig. 3c.

R1336mzz(Z): regarding the 2018 review, three new datasets are available in the literature, totalling 4 papers and 139 data points. McLinden and Akasaka (2020) [32] provide 18 data points in the reduced temperature range $T_r=0.74$ to 0.81 ; the results show good agreement with the reference data from REFPROP10.0, with $AAD\%=0.03\%$ and $MAD\%=0.09\%$. The 17 data from Sakoda et al. (2020) [58] are distributed over a wide temperature range of $T_r=0.65$ to 0.92 , resulting in $AAD\%=0.18\%$ with the same bias, systematic negative deviations from the calculations of REFPROP, and a maximum deviation of $MAD\%=0.36\%$. Li et al. (2020) [60] present an extensive data set of 91 vapour pressures in the temperature range $T_r=0.63$ to 0.99 ; the data are quite scattered with a large increase in deviations at lower temperatures (up to -3% at 278.18 K), $AAD\%=0.23\%$ and $MAD\%=3.00\%$. Results for this fluid are shown in Fig. 3d.

2.2.3 PVT Properties

As shown in Table 3, experimental PVT data are currently available for 17 of the selected refrigerants; for each fluid, these data are listed in Table 7, divided into single-phase and saturated data points, accompanied by the percent absolute average deviation $AAD\%$ of each data set. Looking at the number of papers available, *R1234yf* and *R1234ze(E)* remain the most studied fluids, although, as can be seen from Fig. 1, much effort has been put into the experimental characterisation of *R1336mzz(Z)*, *R1233zd(E)* and *R1224yd(Z)* over the last 4 years; for this reason, a more comprehensive analysis of the peer-reviewed literature published after 2018 is carried out for these 3 fluids and *R1243zf*, exactly as in the previous paragraph.

R1243zf: two new articles were published in relation to the Bobbo et al. (2018) [4] review, for a total of 3 papers and 619 data points.

Figure 4a shows the distribution of the data on the P - T plane, with the pressure shown in logarithmic scale for clarity. On the other hand, Fig. 5a shows the percentage deviations of the experimental data for the fluid from REFPROP.

Compressed liquid: Higashi and Sakoda (2018) [39] reported 28 points in the limited temperature range $T_r=0.87$ to 0.998 and a much wider pressure range $P_r=0.64$ to 1.96 ($P_{\max}=6.73\text{ MPa}$) with $AAD\%=0.29\%$, $MAD\%=1.12\%$ and higher deviations at lower temperatures.

Superheated vapor: Higashi and Sakoda (2018) [39] provided 22 points in the range $T_r=0.87$ to 1.14 and $P_r=0.32$ to 0.995 ($P_{\max}=3.50\text{ MPa}$) with systematic positive deviations from REFPROP 10.0 and higher values at lower temperatures ($AAD\%=0.92\%$, $MAD\%=1.78\%$). Yin et al. (2020) [54] reported 128 density data with $T_r=0.67$ to 0.98 and $P_r=0.03$ to 0.82 ($P_{\max}=2.88\text{ MPa}$); the $AAD\%$ is 0.92% with $MAD\%=1.78\%$ and deviations evenly distributed over the temperature range.

Supercritical region: Higashi and Sakoda (2018) [39] also reported 25 data points in the near-critical region, between $T_r=1.003$ and 1.128 and $P_r=1.040$ to 1.962 . Deviations from REFPROP 10.0 are $AAD\%=0.42\%$ and $MAD\%=1.23\%$, slightly higher at pressures closer to the critical region.

Saturation: Higashi and Sakoda (2018) [39] provided 6 liquid density data and 7 vapour density data in the near critical region $T_r=0.96$ to 0.999 for experimental

Table 7 Available experimental data for the PVT properties of selected refrigerants

ASHRAE designation	References	No. data		T range (K)	P range (MPa)	AAD%
		PpT	P _{sat}			
R1132a	Tomassetti et al. (2021) [10]	131 ^{sv}		223 ÷ 303	0.312 ÷ 2.340	N.A
R1123	Fukushima et al. (2015) [33] Higashi and Akasaka (2016) [34] Akasaka et al. (2020) [17] Kayukawa et al. (2020) [98] Liu et al. (2021) [99] Sakoda et al. (2022) [35]	69 ^{el+sv+scr} 30 ^{el} + 33 ^{sv} 18 ^{el} + 39 ^{sv} + 30 ^{scr} 33 ^{el} + 57 ^{sv}	7 ^l 21 ^{lv}	263 ÷ 473 300 ÷ 430 300 ÷ 430 260 ÷ 400 232 ÷ 303 304 ÷ T _c	1.385 ÷ 9.782 2.252 ÷ 6.675 0.111 ÷ 0.888 0.146 ÷ 7.024 – Up to 6.4	1.99 0.70 1.05 0.67 0.85 N.A
R1132(E)		58 ^{el/sw}	28 ^l + 28 ^v 8 ^v + 10 ^l			
R1234yf	Compressed liquid (cl) Fedele et al. (2012) [100] Klomić et al. (2012a) [101] Qiu et al. (2013) [102] Richter et al. (2011) [19] Tanaka et al. (2010b) [36] Yoshitake et al. (2009) ^{sv} [103]	280 89 128 39 23 73		283 ÷ 353 217 ÷ 353 284 ÷ 363 232 ÷ 365 310 ÷ 360 273 ÷ 323	0.684 ÷ 35.017 0.963 ÷ 40.033 1.000 ÷ 100.000 1.001 ÷ 9.586 1.000 ÷ 5.000 0.800 ÷ 16.000	0.09 0.05 0.16 0.02 0.11 N.A
	Superheated vapor (sv) Di Nicola et al. (2010a) [104] Hu et al. (2017a) [66] Richter et al. (2011) [19] Yin et al. (2019) [71]	136 83 51 172		243 ÷ 373 253 ÷ 346 320 ÷ 400 253 ÷ 368	0.085 ÷ 3.716 0.070 ÷ 1.910 0.554 ÷ 3.252 0.097 ÷ 3.370	0.45 0.19 0.32 0.21
	Supercritical region (scr) Richter et al. (2011) [19]	16		370 ÷ 380	1.021 ÷ 1.947	0.32
	Saturation Tanaka and Higashi (2010a) [36] Hulse et al. (2009) [37]		(1 ^l + 10 ^v) ^{scr} 9 ^l	348 ÷ 368 265 ÷ 365	2.270 ÷ 3.382 0.238 ÷ 3.227	1.17 0.17

Table 7 (continued)

ASHRAE designation	References	No. data		T range (K)	P range (MPa)	AAD%
		PpT	P _{sat}			
R1243zf	Liu et al. (2021) [99]		33 ^v + 33 ^v	227 ÷ 343	–	0.1
	Di Nicola et al. (2013a) [105]	302 ^{el} + 101 ^{sv}		278 ÷ 368	0.260 ÷ 35.000	0.18
	Higashi and Sakoda (2018) [39]	28 ^{el} + 22 ^{sv} + 25 ^{ser}	6 ^l + 7 ^v	328 ÷ 377	1.110 ÷ 6.900	0.66
	Yin et al. (2020) [54]	128 ^{sv}		253 ÷ 268	0.110 ÷ 2.890	0.35
R131I	Duan et al. (1997) [106]	175 ^{sv}		278 ÷ 393	0.190 ÷ 1.750	0.33
	Duan et al. (1999) [40]		32 ^l	302 to T _c	–	8.07
R1234ze (E)	Perera et al. (2022) [41]	47	12 ^v + 12 ^l	301 ÷ 405	0.562 ÷ 6.392	2.19
	Klomfár et al. (2012) [107]	90 ^{el}		208 ÷ 353	1 ÷ 40	0.04
	Compressed liquid (cl)					
	Brown et al. (2012) (CNR-ITC) [108]	270		283 ÷ 353	0.170 ÷ 9.371	0.07
R1234ze (E)	Grebenkov et al. (2009) [43]	20		283 ÷ 371	0.644 ÷ 9.472	0.55
	Klomfár et al. (2012b) [107]	101		205 ÷ 353	1.015 ÷ 40.411	0.04
	McLinden et al. (2010) [81]	42		240 ÷ 380	0.921 ÷ 15.337	0.02
	Qiu et al. (2013) [102]	131		283 ÷ 363	1.000 ÷ 100.010	0.07
	Tanaka et al. (2010a) [83]	26		310 ÷ 370	2.000 ÷ 5.000	0.08
	Yamaya et al. (2011a) [109]	25		270 ÷ 380	2.684 ÷ 16.163	2.96
	Zhang et al. (2020) [110]	97		280 ÷ 331	0.300 ÷ 27.000	0.05
	Superheated vapor (sv)					
	Brown et al. (2012) (UmivPM) [108]	159		243 ÷ 373	0.057 ÷ 1.024	0.63
	Grebenkov et al. (2009) [43]	40		316 ÷ 390	0.570 ÷ 3.649	3.35
McLinden et al. (2010) [81]	40		340 ÷ 420	1.096 ÷ 3.609	0.18	
Tanaka and Higashi (2010b) [111]	204		310 ÷ 360	0.657 ÷ 2.300	0.14	
Yin et al. (2018) [84]	101		313 ÷ 373	0.117 ÷ 2.831	0.11	

Table 7 (continued)

ASHRAE designation	References	No. data	P _{sat}		T range (K)	P range (MPa)	AAD%
			PpT	P _{sat}			
	Zhang et al. (2016a) [112]	26			263 ÷ 293	0.102 ÷ 0.409	0.06
	Supercritical region (scr)						
	McLinden et al. (2010) [81]	54			383 ÷ 420	3.632 ÷ 6.741	0.40
	Yamaya et al. (2011a) [109]	12			385 ÷ 425	4.344 ÷ 15.976	17.64
	Saturation						
	Gong et al. (2016a) [78]			10 ^l	253 ÷ 293	0.097 ÷ 0.430	0.06
	Grebenkov et al. (2009) [43]			7 ^l	251 ÷ 381	0.025 ÷ 0.969	0.14
	Tanaka (2010a) [83]			10 ^l	310 ÷ 370	0.703 ÷ 2.841	0.07
	Higashi et al. (2010) [42]			(9 + 13) ^{v,scp}	368 ÷ 383	2.760 ÷ 3.632	1.49
	Tanaka (2016a) [96]			18 ^l	300 ÷ 380	0.527 ÷ 3.462	0.05
R1225ze(Z)	Brown et al. (2015) [113]		136 ^{cl} + 104 ^{sv}		263 ÷ 368	0.135 ÷ 35.000	N.A
R1336mzz(E)	Tanaka et al. (2017c) [114]		154 ^{sc+sv+sc}	11 ^l + 4 ^v	323 ÷ 523	0.579 ÷ 10.130	N.A
	Sakoda et al. (2021) [44]		24 ^{cl} + 15 ^{sv}	10 ^l + 11 ^v	333 ÷ 410	Up to 5.681	N.A
R1234ze(Z)	Compressed liquid (cl)						
	Fedele et al. (2014b) (CNR-ITC) [85]		313 ^b		283 ÷ 363	0.188 ÷ 34.026	0.09
	Higashi et al. (2015) [45]		38		370 ÷ 432	1.845 ÷ 6.027	0.09
	Romeo et al. (2017) [115]		36		273 ÷ 333	1.000 ÷ 30.050	0.14
	Tanaka et al. (2013a) [116]		41		310 ÷ 410	Up to 5	N.A
	Superheated vapor (sv)						
	Fedele et al. (2014b) (UnivPM) [85]		98		283 ÷ 363	0.082 ÷ 0.436	0.55
	Higashi et al. (2015) [45]		33		360 ÷ 440	0.944 ÷ 4.312	0.34
	Sakoda et al. (2017) [87]		30		353 ÷ 413	0.162 ÷ 2.734	0.11
	Tanaka et al. (2013a) [116]		12		310 ÷ 410	Up to 5	N.A

Table 7 (continued)

ASHRAE designation	References	No. data		T range (K)	P range (MPa)	AAD%
		PpT	P _{sat}			
Saturation						
R1224zd(Z)	Higashi et al. (2015) [45]		9 ^l + 10 ^v	356 ÷ 423	0.925 ÷ 3.531	2.24
	Kayukawa et al. (2012)a [86]		111	310 ÷ 410	0.263 ÷ 2.780	N.A
	Tanaka (2016a) [82]		22 ^l	300 ÷ 400	0.186 ÷ 2.309	0.18
	Sakoda and Higashi (2019) [47]	16 ^{cl} + 30 ^{sv}	9 ^l + 8 ^v	330 ÷ 429	0.361 ÷ 6.410	0.59
	Fedele et al. (2020) [94]	93 ^{cl}	9 ^l	283 ÷ 363	< 35	0.04
R1354mzy(E)	Lago et al. (2022) [95]	80 ^{cl}		273 ÷ 353	1 ÷ 35	0.03
	Kayukawa et al. (2015)a [117]	50 ^{cl}		280 ÷ 420	1.000 ÷ 20.000	N.A
	Kimura et al. (2017a) [90]	10 ^{ncp} + 21 ^{scr}		425 ÷ 450	3.249 ÷ 5.056	N.A
	Kimura et al. (2017b) [90]	50 ^{cl} + 52 ^{sv}		280 ÷ 420	0.482 ÷ 20.000	N.A
R1233zd(E)	Compressed liquid (cl)					
	Fedele et al. (2018) (CNR-ITC) [118]	93		283 ÷ 363	0.133 ÷ 35.002	0.04
	Mondejar et al. (2015) [30]	117		215 ÷ 444	0.476 ÷ 24.079	0.01
	Romeo et al. (2017) [115]	30		274 ÷ 333	1.000 ÷ 25.010	0.02
	Tanaka (2016b) [96]	39		329 ÷ 440	0.777 ÷ 9.765	0.65
	Superheated vapor (sv)					
Fedele et al. (2018) (UnivPM) [118]	60		308 ÷ 373	0.167 ÷ 0.693	0.41	
Mondejar et al. (2015) [30]	43		350 ÷ 440	0.255 ÷ 1.923	0.05	
Tanaka (2016b) [96]	33		328 ÷ 443	0.777 ÷ 9.770	7.74	
Yin et al. (2021) [59]	63		303 ÷ 373	0.091 ÷ 0.990	0.10	
Supercritical region (scr)						
Mondejar et al. (2015) [30]	5		444	3.858 ÷ 5.619		0.02
Tanaka (2016b) [96]	25		440 ÷ 444	3.773 ÷ 8.632		2.02

Table 7 (continued)

ASHRAE designation	References	No. data		T range (K)	P range (MPa)	AAD%
		PpT	P_{sat}			
Saturation						
	Hulse et al. (2012) [50]		13 ^l	243 ÷ 293	0.011 ÷ 0.108	0.15
	Tanaka et al. (2016a) [92]		11 ^l	300 ÷ 400	0.136 ÷ 1.793	0.21
R1354myf(E)	Kayukawa et al. (2015) ^a [117]	47 ^{cl}		280 ÷ 420	0.480 ÷ 20.000	N.A
R1336mzz(Z)	Tanaka et al. (2016) [119]	278 ^{sl+sv} + 66 ^{tep}	11 ^l + 4 ^v	323 ÷ 503	0.182 ÷ 9.927	N.A
	Sun et al. (2019) [97]	137 ^{cl}		283 ÷ 373	< 100	0.03
	McLinden and Akasaka (2020) [32]	97 ^{cl} + 1 ^{sv} + 7 ^{scr}		230 ÷ 460	0.790 ÷ 4.740	0.02
R1130(E)	Tanaka et al. (2022) [13]	21 ^{cl} + 52 ^{sv}	8 ^v + 6 ^l	326 ÷ 408	0.111 ÷ 10.525	N.A
RE356mmz	Chen et al. (2020) [120]	105 ^{sv}		333 ÷ 451	0.105 ÷ 2.000	N.A
	Kano (2020) [121]	25 ^{sv}		343 ÷ 423	0.051 ÷ 0.703	N.A
	Chen et al. (2020) [122]	164 ^{cl}		313 ÷ 448	0.414 ÷ 25.002	N.A

Properties are in bold

AAD relative to the EOS cited in Table 4

^{cl}Compressed liquid

^{sv}Superheated vapor

^{scr}Supercritical conditions

^{nep}Near critical point

^lLiquid

^vVapor

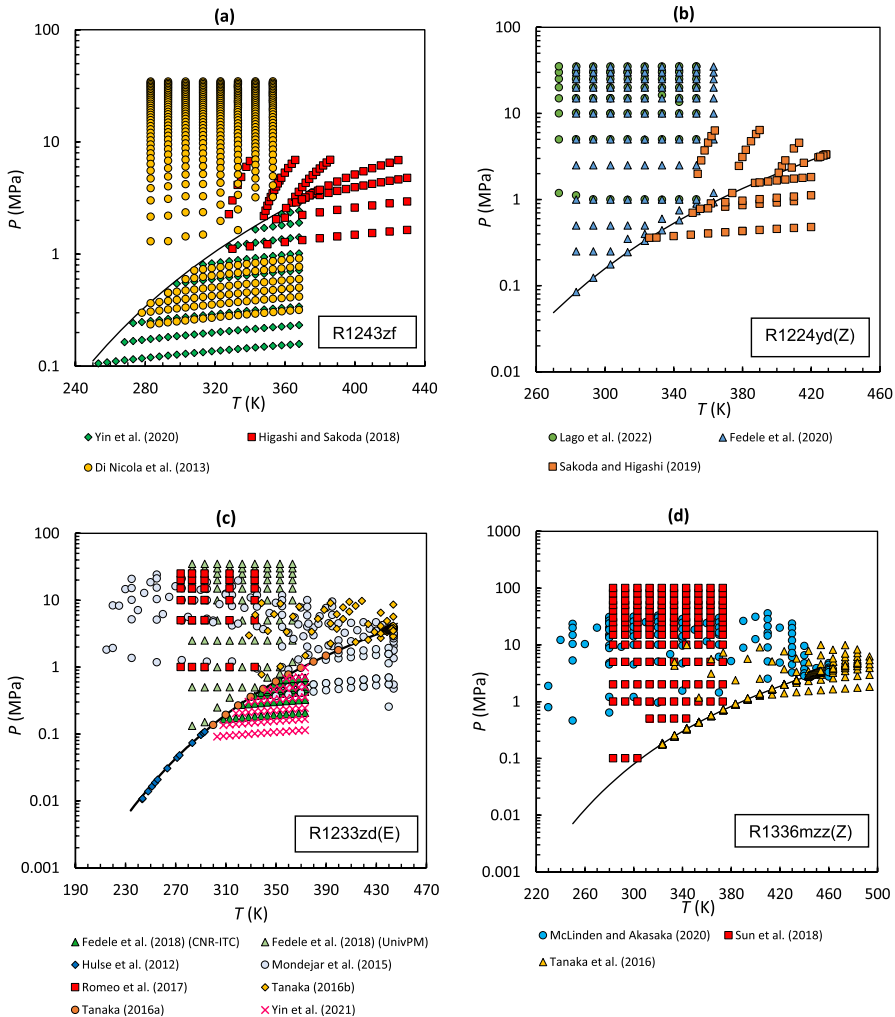


Fig. 4 Distribution on the P–T plane of the available experimental PVT data for (a) R1243zf, (b) R1224yd(Z), (c) R1233zd(E) and (d) R1336mzz(Z). Solid line: pressure curve. x: critical point

characterisation of critical density. The deviations are $AAD\% = 0.97\%$ and $MAD\% = 2.91\%$.

R1224yd(Z): 3 data sets with a total of 245 data points were identified in the literature: all four sets contain compressed liquid data, 1 superheated vapour data, 1 saturated vapour data and 2 saturated liquid data. Figures 4b and 5b show the distribution of the data on the P–T plane and the percentage deviations of the experimental data for the fluid from REFPROP, respectively.

Compressed liquid: the 16 data from Sakoda and Higashi (2019) [47] exhibit small deviations over the entire temperature and pressure range ($T_r = 0.83$ to 0.94 and $P_r = 0.59$ to 1.92, $P_{max} = 6.41$ MPa), with $AAD\% = 0.08\%$ and

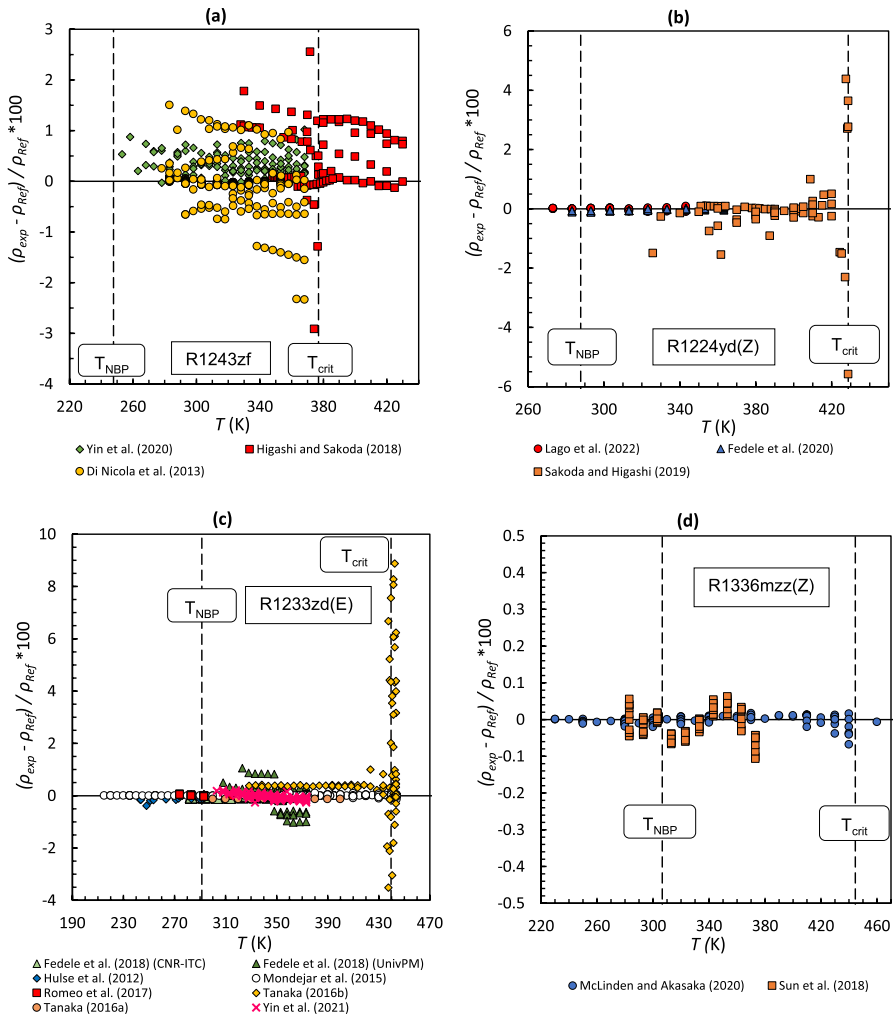


Fig. 5 Deviations of the experimental PVT data for (a) R1243zf, (b) R1224yd(Z), (c) R1233zd(E) and (d) R1336mzz(Z) from the values calculated using REFPROP 10.0

MAD% = 0.28%. Fedele et al. (2020) [94] provided 93 density data in the medium temperature range $T_r = 0.66$ to 0.85 and the much wider pressure range $P_r = 0.075$ to 10.507 ; the deviations are really small: AAD% = 0.046% and MAD% = 0.12%. However, it must be considered that 4 data points were excluded because they are outside the validity range of the EoS used in REFPROP. Finally, Lago et al. (2022) [95] presented 80 data points, 9 of which exceed the validity range of the EoS implemented in REFPROP, in the range $T_r = 0.64$ to 0.94 and $P_r = 0.29$ to 10.55 ($P_{max} = 35$ MPa); the agreement with the reference data from REFPROP is excellent, with AAD% = 0.03% and MAD% = 0.098%.

Superheated vapor: Sakoda and Higashi (2019) [47] present 30 data in the range $T_r=0.77$ to 0.98 for pressures $P_r=0.11$ to 0.55 ($P_{\max}=35$ MPa); deviations are higher than those of the data for compressed liquid, with AAD% 0.19% and MAD% $=0.57\%$.

Saturation: the 17 data from Sakoda and Higashi (2019) [47] includes data points for saturated liquid and 8 for saturated vapour in the range $T_r=0.82$ to 1.00 , with high deviations increasing with temperatures: AAD% $=1.804\%$ and MAD% $=5.57\%$. Fedele et al. (2020) [94] presented 9 points for saturated liquid from $T_r=0.66$ to $T_r=0.85$; the deviations are low in the whole temperature range (AAD% $=0.04\%$, MAD% $=0.07\%$).

R1233zd(E): a total of 532 data points and 7 papers are reported for this fluid; compressed liquid data, as well as superheated vapour data are contained in 4 of the 7 papers. 2 papers contain data for the supercritical region and 2 contain data for the saturated region. With reference to Bobbo et al. (2018) [4], 2 papers are added to this review and are discussed in the following lines.

Figure 4c shows the distribution of the data on the P–T plane, while Fig. 5c shows the percentage deviations of the experimental data for the fluid from REFPROP.

Superheated vapour: Yin et al. (2021) [59] collected 63 points for the superheated vapour in the range $T_r=0.69$ to 0.85 , $P_r=0.03$ to 0.28 ($P_{\max}=0.99$ MPa); the data are a little scattered between positive and negative deviations, but still show a great agreement with the reference data from REFPROP (AAD $=0.10\%$, MAD% $=0.27\%$).

Saturation: the 11 points for saturated liquid from Tanaka et al. (2016a) [96] examine the temperature range $T_r=0.68$ to 0.91 , and show constant deviations for each point with AAD% $=0.21\%$ and MAD% $=0.24\%$.

R1336mzz(Z): two new studies were published for this fluid after the publication of Bobbo et al. (2018) [4], which are described in more detail below. They come to a total of 601 data points and three papers: all of them report compressed liquid data, 2 report superheated vapour data, one reports near critical point data and one reports supercritical data. As with the previous fluids, Figs. 4d and 5d show the data distribution on the P–T plane and the percentage deviations of the experimental data for the fluid from REFPROP, respectively.

Compressed liquid: the Sun et al. (2019)[97] paper contains 137 density data distributed in the medium temperature range $T_r=0.64$ to 0.84 and a much wider pressure range $P_r=0.035$ to 34.55 ; the maximum reported pressure is 100 MPa, exceeding the validity range of the EoS used in REFPROP ($P_{\max}=46$ MPa), so 40 points were excluded from the analysis. The data showed good agreement with REFPROP, with AAD% $=0.03\%$ and MAD% $=0.11\%$. Then McLinden and Akasaka (2020)[32] provided 97 data points in the wider temperature range $T_r=0.52$ to 0.99 for pressures $P_r=0.22$ to 12.33 ($P_{\max}=35.70$ MPa); again, the agreement with the reference data was excellent (AAD% $=0.01\%$ and MAD% $=0.07\%$).

Superheated vapor: McLinden and Akasaka (2020) [32] also reported 1 point under superheated vapor conditions, close to the critical point ($T_r=1.035$, $P_r=0.95$, $P=2.74$ MPa), with AAD% 0.007% .

Finally, supercritical: McLinden and Akasaka (2020) [32] identified 7 data near the critical point with $T_r=1.01$ to 1.03 and $P_r=1.14$ to 1.64 , showing higher

deviations compared to the compressed liquid and superheated vapour regions, i.e., $AAD\% = 0.13\%$ and $MAD\% = 0.26\%$.

2.2.4 Specific Heat Capacity

Specific heat capacity measurements are only available for seven of the selected fluids, which turns out to be the least studied property among those considered in this work. Table 8 summarises the available data sets and distinguishes between data related to isochoric heat capacity in the single-phase region (c_v), ideal gas capacity (c_p^0), isobaric heat capacity under saturated conditions ($c_{p\text{ sat}}$) and in the single-phase region (c_p), the latter being the most frequently measured among the heating properties; as can be seen from the Table, R1234yf and R1234ze(E) are also the most studied fluids for this property, while for two of the four fluids on which this study focuses, i.e., R1243zf and R1224yd(Z), no data are available at all. On the other hand, three new papers have recently been published for R1233zd(E) and R1243zf:

R1243zf: a total of two papers and 150 data points are now available, both regarding directly measured isochoric heat capacity in the compressed liquid region. Sheng et al. (2021) [123] report 64 isochoric heat capacities with systematic negative deviations and $AAD\% = 2.35\%$, $MAD\% = 3.82\%$, which perfectly matches the 86 data presented by Ding et al. (2021) [123] ($AAD\% = 2.36\%$, $MAD\% = 4.34\%$). The distribution of the available data on the P–T plane and the deviations from REFPROP are shown in Figs. 6a and 7a, respectively.

R1233zd(E): after the publication of the review paper by Bobbo et al. (2018) [4], only the paper by Liu et al. (2018) [124] was presented, which contains 63 isobaric heat capacities in the compressed liquid and supercritical regions. The deviations are quite significant, especially at higher pressures and temperatures close to the critical region ($AAD\% = 5.13\%$, $MAD\% = 10.28\%$). The distribution of the available data and the deviations from REFPROP are shown in Figs. 6b and 7b, respectively.

2.2.5 Speed of Sound

As far as the speed of sound is concerned, the number of analysed fluids has more than doubled compared to the last review, for a total of eleven fluids, namely R1234ze (E), R1234yf, R1233zd(E), R1234ze(Z), R1336mzz(Z), R1224yd(Z), R1243zf, R1336mzz(E), R1311, R1123 and RE356mmz. For all these fluids speed of sound data are listed in Table 9.

For *R1243zf* and *R1224yd(Z)*, one data set each is available in the peer-reviewed literature, both for the superheated vapour phase. Kano et al. (2020) [141] provided 36 data for the vapour phase speed of sound of R1224yd(Z), with reduced temperatures between 0.71 and 0.82 and reduced pressures between 0.04 and 0.20: deviations from REFPROP are small in all these ranges, with $AAD\% = 0.01$ and $MAD\% = 0.04$. On the other hand, Chen et al. (2021) [142] measured the vapour phase speed of sound of R1243zf (92 data) in the ranges $T_r = 0.83$ to 0.96 and $P_r = 0.05$ to 0.28. Deviations from REFPROP are systematically negative and higher for conditions further from the critical region ($AAD\% = 0.198$, $MAD\% = 0.44$).

Table 8 Available experimental data for the heat capacity of selected refrigerants

ASHRAE designation	References	No. data							
		c_p^0	c_p	$c_{p, sat}$	c_v	T range (K)	P range (MPa)		
R1132a	Low (2018) [15]	–	–	20	–	193 ÷ 288	–		
R1234yf	Gao et al. (2014a) [125]	–	74 ^l	11 ^{lb}	–	305 ÷ 355	1.500 ÷ 5.000		
	Hulse et al. (2009) [37]	13	–	–	–	213 ÷ 573	–		
	Kano et al. (2010) [126]	6 ^a	–	–	–	278 ÷ 353	–		
	Liu et al. (2017) [127]	–	154 ^{d+scr}	–	–	304 ÷ 373	1.510 ÷ 12.080		
	Tanaka et al. (2010b) [128]	–	22 ^{cl}	6 ^l	–	310 ÷ 360	0.940 ÷ 5.000		
	Kagawa and Matsuguchi (2020) [129]	–	62	5 ^b	–	289 ÷ 353	0.300 ÷ 2.200		
	Lu kawski et al. (2018) [130]	–	33 ^{scr}	–	–	373 ÷ 413	3.500 ÷ 10.000		
	Zhong et al. (2018) [131]	–	–	–	74	240 ÷ 341	< 13.000		
	Sheng et al. (2022) [132]	–	33	–	–	230 ÷ 285	up to 8.000		
R1243zf	Sheng et al. (2021) [133]	–	–	–	64 ^{cl}	299 ÷ 351	1.600 ÷ 11.000		
	Ding et al. (2021) [123]	–	–	–	86 ^{cl}	250 ÷ 300	1.600 ÷ 10.000		
	Duan et al. (1997) [134]	–	–	–	–	273 ÷ 333	–		
R131I	Gao et al. (2015) [135]	10 ^a	–	–	–	310 ÷ 365	1.560 ÷ 5.490		
R1234ze (E)	Kagawa et al. (2011) [136]	–	95 ^{cl}	12 ^{lb}	–	303 ÷ 363	0.350 ÷ 1.300		
	Kano et al. (2013) [137]	–	19 ^{sv}	–	–	278 ÷ 353	–		
	Liu et al. (2018) [138]	6 ^a	–	–	–	313 ÷ 393	1.040 ÷ 10.090		
	Tanaka et al. (2010c) [128]	–	130 ^{d+scr}	–	–	310 ÷ 370	2.000 ÷ 5.000		
	Yamaya et al. (2011a) [139]	–	26 ^{cl}	7 ^{lb}	–	270 ÷ 425	2.684 ÷ 15.976		
	Wang et al. (2020) [140]	–	–	–	37 ^{cl}	237 ÷ 349	1.600 ÷ 9.200		
	Sheng et al. (2022) [132]	–	57	–	–	232 ÷ 339	1.900 ÷ 8.100		

Table 8 (continued)

ASHRAE designation	References	No. data					T range (K)	P range (MPa)
		c_p^0	c_p	$c_{p, \text{sat}}$	c_v			
R123zd(E)	Hulse et al. (2012) [50] Liu et al. (2018) [124]	11 ^c	—	—	—	100 ÷ 1000	—	
RE356mmz	Kano (2020) [141]	5 ^a	63 ^{el+scr}	—	—	313 ÷ 445 343 ÷ 423	1.000 ÷ 10.000 —	

^aDerived from speed of sound measurements

^bCalculated by extrapolation of c_p to saturation pressure

^cCalculated with quantum mechanics

^{el}Compressed liquid

^{sv}Superheated vapor

^{scr}Supercritical conditions

^lLiquid

^vVapor

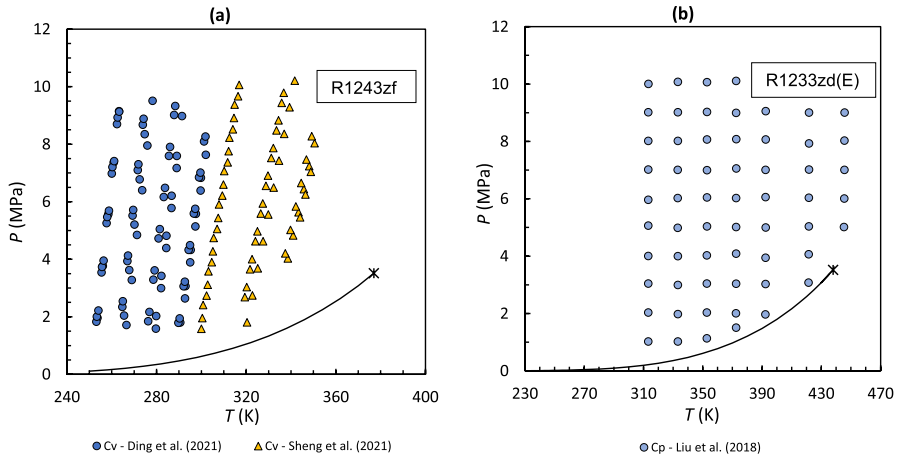


Fig. 6 Distribution on the P–T plane of the available specific isobaric and isochoric heat capacity data for (a) R1243zf and (b) R1233zd(E). Solid line: pressure curve. x: critical point

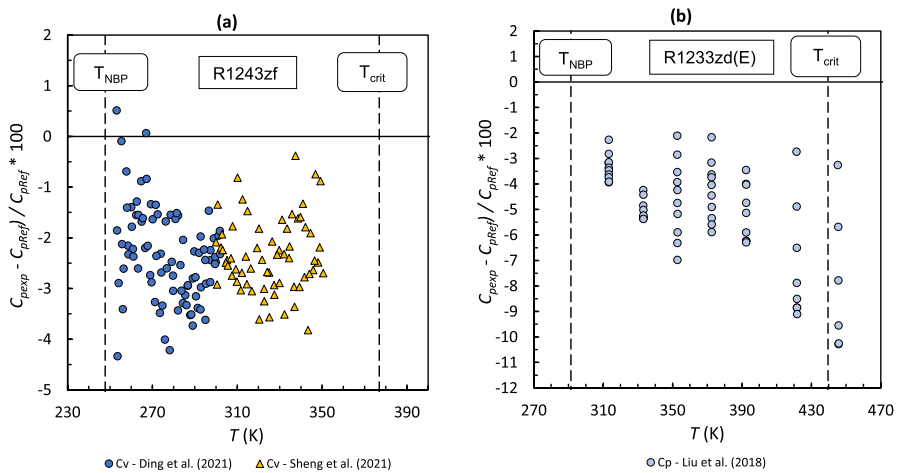


Fig. 7 Deviations of the experimental specific isobaric and isochoric heat capacity data for (a) R1243zf and (b) R1233zd(E) from the values calculated using REFPROP 10.0

R1233zd(E) is now the most studied fluid, with a total of 461 points and 5 data sets, three of which were not included in the previous review, one for the compressed liquid and two for the superheated vapour: Lago et al. (2018) [143] reported 43 data for compressed liquid in the ranges $T_r=0.62$ to 0.80 , $P_r=0.08$ to 9.28 ; the deviations from REFPROP are $AAD\%=0.18$ and $MAD\%=0.35$, slightly higher for lower temperatures. On the other hand, Kano (2021) [144] and Peng et al. (2022) [145] have both recently presented data for the compressed liquid, 36 and 92 data points, respectively: Kano (2021) [144] data range from 0.71 to 0.92 for T_r and 0.08 to 0.24 for P_r and show higher deviations from REFPROP for temperatures

Table 9 Available experimental data for the speed of sound of selected refrigerants

ASHRAE designation	Reference	No. data	T range (K)	P range (MPa)	AAD%
R1123	Kano et al. (2020) [141]	48 ^{sv}	263 ÷ 333	0.050 ÷ 0.520	0.05
R1234yf	Gao et al. (2014b) [146]	N.A	273 ÷ 353	0.316 ÷ 2.520	N.A
	Kano et al. (2010) [126]	41 ^{sv}	278 ÷ 353	0.025 ÷ 0.407	0.01
	Lago et al. (2011) [147]	22 ^{cl}	260 ÷ 360	1.990 ÷ 6.060	0.19
	McLinden and Perkins (2018) [148]	86 ^{cl}	235 ÷ 380	0.637 ÷ 25.751	0.7
R1243zf	Chen et al. (2021) [142]	92 ^{sv}	313 ÷ 363	0.170 ÷ 0.983	0.2
R131I	Duan et al. (1997) [134]	67 ^{sv}	273 ÷ 333	0.058 ÷ 0.276	0.08
R1234ze (E)	Kano et al. (2013) [137]	41 ^{sv}	278 ÷ 353	0.025 ÷ 0.403	0.04
	Lago et al. (2011) [147]	24 ^{cl}	260 ÷ 360	1.960 ÷ 10.110	0.23
	McLinden and Perkins (2018) [148]	134 ^{cl}	230 ÷ 420	0.898 ÷ 36.704	0.04
	Perkins and McLinden (2015) [149]	223 ^{sv}	280 ÷ 420	0.080 ÷ 2.832	0.6
R1336mzz(E)	Peng et al. (2022) [145]	98 ^{sv}	298 ÷ 363	0.120 ÷ 0.805	–
R1234ze(Z)	Lago et al. (2016) [150]	38 ^{cl}	273 ÷ 333	0.192 ÷ 25.059	3.9
	Lozano Martin et al. (2019) [151]	94 ^{sv}	307 ÷ 420	< 1.800	0.01
	Peng et al. (2022) [145]	58 ^{sv}	303 ÷ 363	0.129 ÷ 0.730	0.18
R1224yd(Z)	Kano et al. (2020) [141]	36 ^{sv}	303 ÷ 353	0.040 ÷ 0.204	0.01
R1233zd(E)	McLinden and Perkins (2018) [139]	135 ^{cl}	230 ÷ 420	0.135 ÷ 25.613	0.61
	Mondejar et al. (2015) [30]	155 ^{sv}	290 ÷ 420	0.068 ÷ 2.073	0.06
	Lago et al. (2018) [143]	43 ^{cl}	273 ÷ 353	1.000 ÷ 35.000	0.18
	Kano (2021) [144]	36 ^{sv}	313 ÷ 403	0.030 ÷ 0.377	0.11
	Peng et al. (2022) [145]	92 ^{sv}	313 ÷ 363	0.120 ÷ 0.550	0.005
	McLinden and Akasaka (2020) [32]	140 ^{cl}	280 ÷ 480	0.020 ÷ 2.200	0.02
R1336mzz(Z)	McLinden and Perkins (2018) [148]	183 ^{cl}	230 ÷ 420	0.674 ÷ 45.530	–
	Kano (2020) [121]	25 ^{sv}	343 ÷ 423	0.051 ÷ 0.703	–

AAD relative to the EOS cited in Table 4

^{cl}Compressed liquid^{sv}Superheated vapor

and pressures further from the critical point (AAD% = 0.11, MAD% = 0.24), while the data of Peng et al. (2022) [145] exhibit very small absolute deviations throughout the temperature and pressure range ($T_r = 0.71$ to 0.83, $P_r = 0.12$ to 0.15), with AAD% = 0.005 and MAD% = 0.02.

Finally, two speed of sound data sets are available for *R1336mzz(Z)* so far, one published by McLinden and Akasaka (2020) [32] published after the 2018 review: the study reports 140 speed of sound data in the liquid phase in the ranges $T_r = 0.72$ to 1.08 and $P_r = 0.01$ to 0.70; the data are quite scattered between

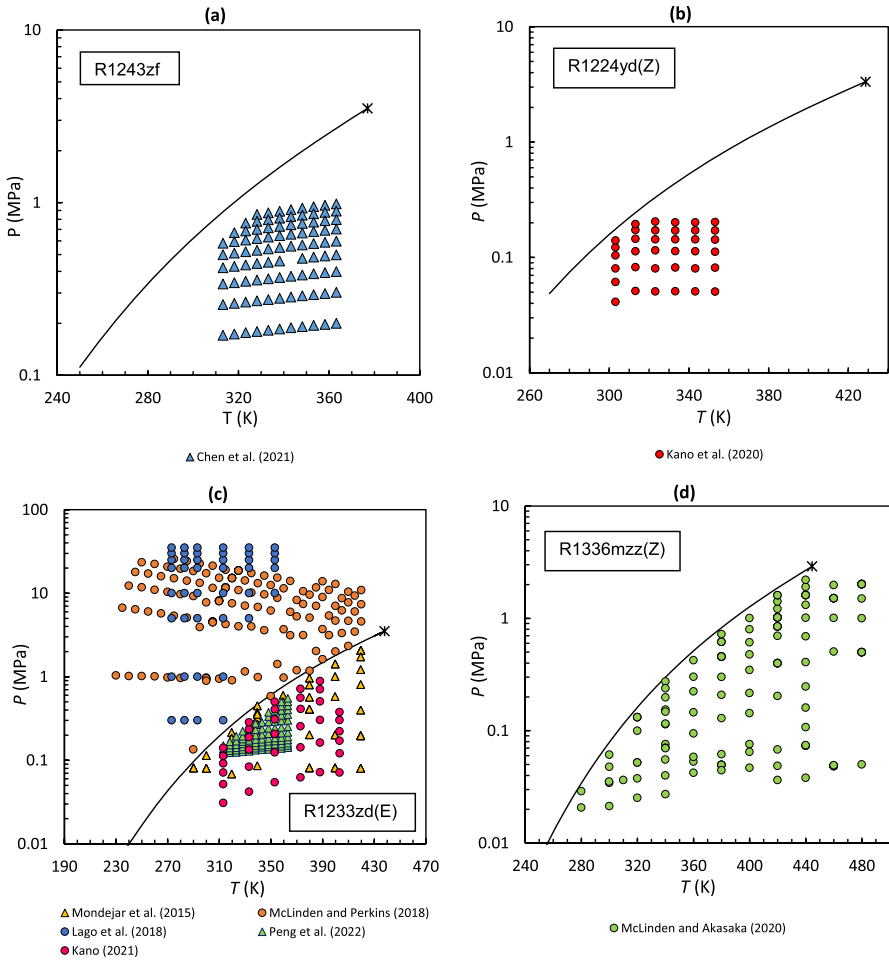


Fig. 8 Distribution on the P–T plane of the available speed of sound data for (a) R1243zf, (b) R1224yd(Z), (c) R1233zd(E) and (d) R1336mzz(Z). Solid line: pressure curve. x: critical point

positive and negative deviations, with no significant trend in temperature or pressure. Overall, excellent agreement with the reference data from REFPROP can be observed (AAD% = 0.02, MAD% = 0.08).

For all four fluids Fig. 8 shows the distribution of the available data on the P–T plane, while Fig. 9 gives the deviations from REFPROP.

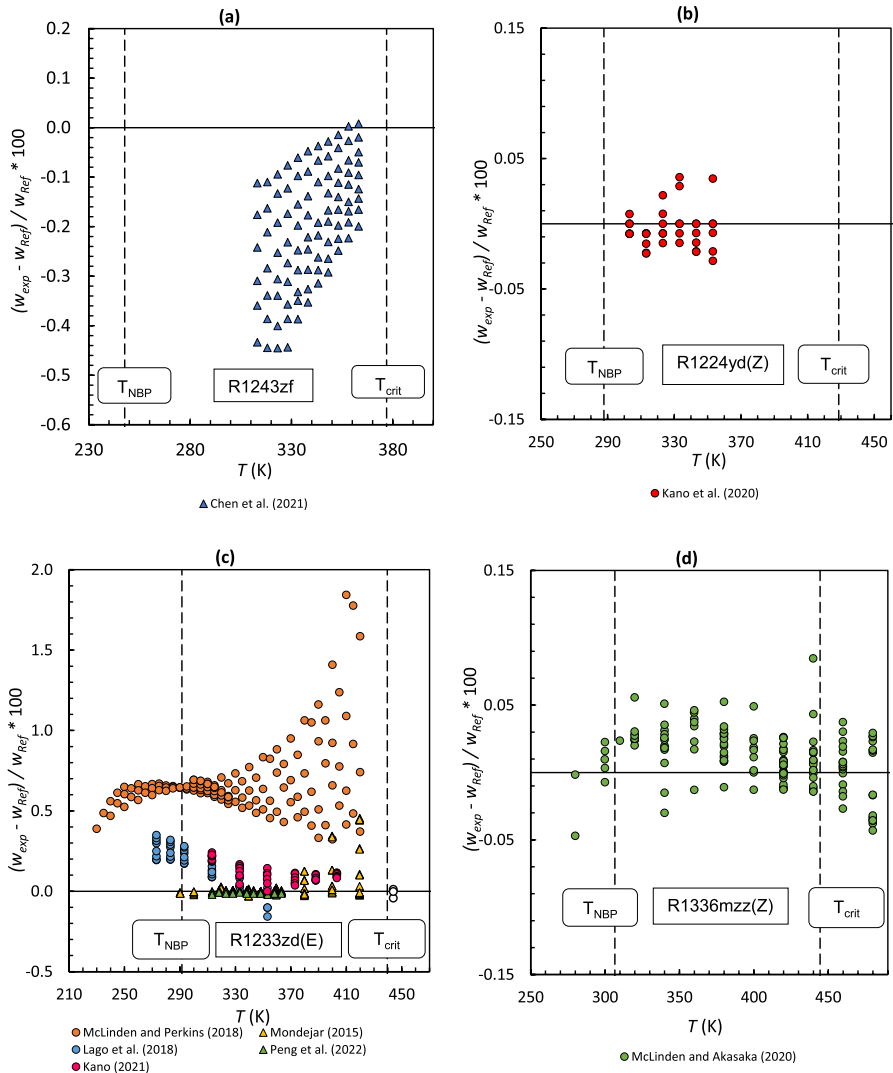


Fig. 9 Deviations of the experimental speed of sound data for (a) R1243zf, (b) R1224yd(Z), (c) R1233zd(E) and (d) R1336mzz(Z) from the values calculated using REFPROP 10.0

2.3 Transport Properties

2.3.1 Thermal Conductivity

Experimental measurements of thermal conductivity have increased by 300% in the last 4 years: while only 3 working fluids were studied in 2018, this number has now increased to 9, including R1234ze(E), R1234yf, R1233zd(E), R1234ze(Z), R1336mzz(Z), R1224yd(Z), R1243zf, R1336mzz(E) and RE356mmz. For all these

fluids the publicly available thermal conductivity data are listed in Table 10, divided into single-phase data and saturated data. As for the four fluids R1336mzz(Z), R1233zd(E), R1243zf and R1224yd(Z), 2 publications are available for each of R1336mzz(Z) and R1233zd(E), while only one thermal conductivity data set is available for each of the other fluids. As no thermal conductivity data were available for R1243zf and R1224yd(Z) prior to this paper, reference values calculated with REFPROP 10.0 are based on an extended corresponding states model in predictive mode [152], with an estimated uncertainty of 20% for both liquid and vapor phases.

R1243zf: Kim et al. (2021) [153] recently reported 35 thermal conductivity data for R1243zf in both the compressed liquid (25 data from 314.2 K to 374.7 K and from 2 MPa to 6 MPa) and the superheated vapor (10 data from 355.7 K to 405.6 K and pressures from 0.9 MPa to 3.4 MPa) regions, with a maximum reported uncertainty of 2%. Deviations between experimental and calculated data from REFPROP are $AAD\% = 4.22$ and $MAD\% = 13.74$.

R1224yd(Z): for R1224yd(Z) a total of 112 data were measured by Alam et al. (2019) [12], 66 data points for the compressed liquid (in the ranges $T = 317$ K to 416 K and $P = 1.0$ to 4.0 MPa, declared uncertainty: max 2.1%), and 46 for the superheated vapor ($T = 376$ K to 453 K, $P = 0.2$ to 1.5 MPa, declared uncertainty: max 2.3%). Deviations from REFPROP reference values are $AAD\% = 4.49$ and $MAD\% = 8.58$.

R1233zd(E): a total of 2537 data were reported for R1233zd(E). Perkins et al. (2017) [154] measured the thermal conductivity in both the compressed liquid (1453 data), superheated vapor (635 data) and supercritical (316 data) regions in the ranges of 204 K to 453 K for temperature and 0.1 MPa to 67 MPa for pressures; based on these experimental data the correlation implemented in REFPROP was formulated, and deviations from the calculated values are $AAD\% = 0.82$ and $MAD\% = 6.00$. Alam et al. (2018) [155] performed 115 measurements, both in the compressed liquid region (64 data points for the temperature range from 313 K to 433 K, pressures from 1.01 MPa to 4.02 MPa) and in the superheated vapor region (51 data points for the temperature range from 334 K to 474 K, pressures up to 4 MPa). This data set is in good agreement with the one from Perkins et al. (2017), and deviations from reference values are $AAD\% = 0.92$ and $MAD\% = 2.98$.

R1336mzz(Z): finally, a total of 3460 thermal conductivity data are reported for R1336mzz(Z), which is by far the most investigated fluid: Alam et al. (2017) [156] measured the thermal conductivity both in the compressed liquid region (74 data, temperatures from 314 K to 435 K) and superheated vapor region (92 data, temperatures from 321 K to 96 K) for pressures lower than 4 MPa; based on these data the correlation implemented in REFPROP 10.0 was made, with an estimated uncertainty of 3% along saturation and in gas phase, and higher at higher pressures and near critical point. Perkins and Huber (2020) [157] gathered a huge dataset of 3294 data points, 1167 for the compressed liquid phase ($T = 192$ K to 428 K, declared uncertainty: 1%), 1323 for the superheated vapor phase ($T = 303$ K to 444 K, declared uncertainty: 1.5%), and 804 for the supercritical region ($T = 457$ K to 498 K, declared uncertainty: 1%). Deviations from REFPROP, shown in Fig. 11d, are $AAD\% = 5.93$ and $MAD\% = 16.71$. Measurements were performed at pressures up to 69 MPa: since the correlations implemented in REFPROP for this fluid is only

Table 10 Available experimental data for the thermal conductivity of selected refrigerants

ASHRAE designation	References	No. data		T range (K)	P range (MPa)
		λ	λ_{sat}		
R1234yf	Perkins and Huber (2011) [158]	31 ^{cl} + 479 ^{sv}	–	242 ÷ 344	0.10 ÷ 23.00
R1243zf	Kim et al. (2021) [153]	25 ^l + 10 ^v	–	313 ÷ 406	0.17 ÷ 3.40
R1234ze (E)	Perkins and Huber (2011) [158]	452 ^{cl} + 451 ^{sv}	–	203 ÷ 344	0.10 ÷ 23.00
R1336mzz(E)	Grebekov et al. (2009) [43]	94 cl + 84 ^{sv}	–	252 ÷ 407	0.05 ÷ 20.00
	Mondal et al. (2021) [159]	86 ^l + 94 ^v + 28 ^{scr}	–	313 ÷ 453	0.50 ÷ 4.00
	Haowen et al. (2021) [160]	–	55 ^l	253 ÷ 353	–
R1234ze(Z)	Ishida et al. (2015) [161]	–	21 ^l + 24 ^v	283 ÷ 353	–
R1224yd(Z)	Alam et al. (2019) [162]	66 ^l + 46 ^v	–	317 ÷ 453	1.00 ÷ 4.00
R1233zd(E)	Alam et al. (2018) [155]	64 ^{cl} + 51 ^{sv}	–	313 ÷ 474	1.01 ÷ 4.02
R1336mzz(Z)	Perkins et al. (2017) [154]	1453 ^{cl} + 635 ^{sv} + 316 ^{scr}	–	204 ÷ 453	0.10 ÷ 67.00
	Perkins and Huber (2020) [157]	1167 ^l + 1323 ^v + 804 ^{scr}	–	192 ÷ 498	< 69.00
RE356mmz	Alam et al. (2017) [156]	74 ^l + 92 ^v	–	314 ÷ 496	< 4.00
	Alam et al. (2019) [12]	96 ^l + 30 ^v	–	319 ÷ 452	0.18 ÷ 4.00

^{cl}Compressed liquid

^{sv}Superheated vapor

^{scr}Supercritical conditions

^lLiquid

^vVapor

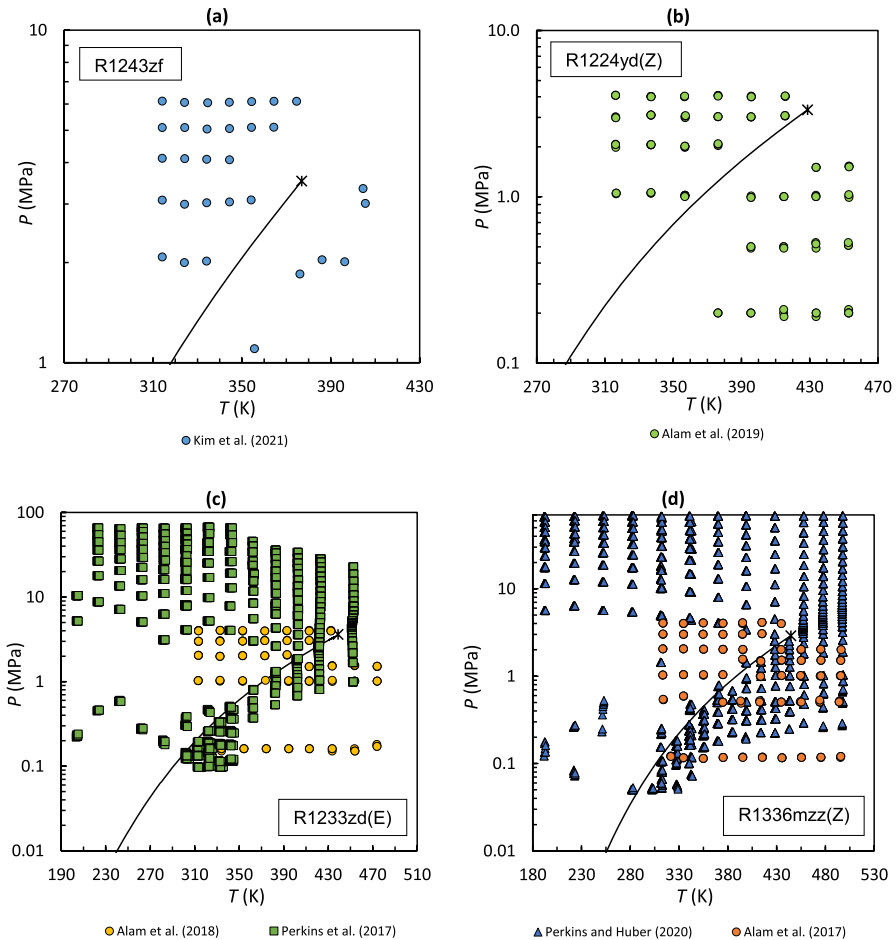


Fig. 10 Distribution on the P–T plane of the available thermal conductivity data for (a) R1243zf, (b) R1224yd(Z), (c) R1233zd(E) and (d) R1336mzz(Z). Solid line: pressure curve. x: critical point

valid up to 46 MPa the authors provided a supplementary file to extend its range of validity up to 69 MPa.

Figure 10a, b, c, d displays the distribution of thermal conductivity data on the P–T plane, while Fig. 11a, b, c, d shows the deviations from REFPROP 10.0.

2.3.2 Viscosity

To date, experimental viscosity data for nine of the selected fluids have been published in the literature and are listed here in Table 11. As shown in Fig. 1, R1234yf is still the most studied working fluid, followed by R1233zd(E), for which four new sets of viscosity data have been published since 2018. The distribution of available data on the P–T plane for the four fluids R1243zf, R1224yd(Z), R1233zd(E)

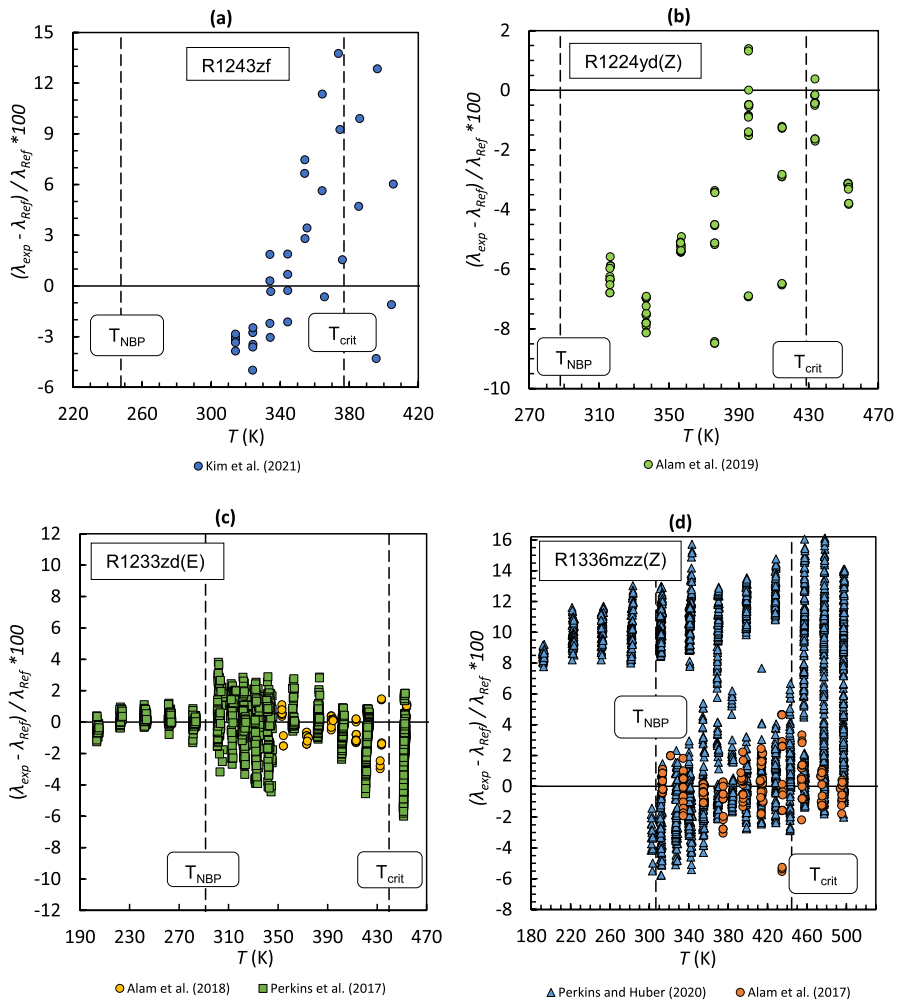


Fig. 11 Deviations of the experimental thermal conductivity data for (a) R1243zf, (b) R1224yd(Z), (c) R1233zd(E) and (d) R1336mzz(Z) from the values calculated using REFPROP 10.0

and R1336mzz(Z) is shown in Fig. 12a, b, c, d, while Fig. 13a, b, c, d shows the deviations from the reference data from REFPROP. It must be underlined that since before 2018 no viscosity data were available for these fluids, except from the data set from Hulse et al. (2012) [50], values provided in REFPROP 10.0 are calculated with an ECS and different estimated uncertainties depending on the fluid [152].

R1243zf: only the data set by Zhao et al. (2021) [163] is available today, which reports 12 data for saturated liquid kinematic viscosity and presents deviations higher than 10% at higher temperatures ($MAD\% = 13.25$ at 372.84 K).

R1224yd(Z): 2 data sets are available (totalling 136 viscosity data), all published after 2018, both containing data in single phase regions. Miyara et al.

Table 11 Available experimental data for the viscosity of selected refrigerants

ASHRAE designation	Reference	No. data	<i>T</i> range (K)	<i>P</i> range (MPa)
R1234yf	Cousins and Laesecke (2012) [170]	20 ^{sat l}	247 ÷ 340	0.115 ÷ 1.911
	Dang et al. (2015a) [171]	25 ^{cl}	283 ÷ 321	0.591 ÷ 1.302
	Dang et al. (2015b) [172]	8 ^{sv}	274 ÷ 338	0.105
	Hulse et al. (2009) [37]	39 ^{cl}	257 ÷ 307	0.326 ÷ 2.109
	Meng et al. (2013) [173]	110 ^{cl}	243 ÷ 363	Saturation ÷ 30.000
	Yamaguchi et al. (2009) ^a [174]	94	263 ÷ 323	0.100 ÷ 1.960
	Zhao et al. (2014) [175]	10 ^{satl}	293 ÷ 365	At saturation
R1243zf	Zhao et al. (2021) [163]	12 ^{satl}	303 ÷ 432	0.150 ÷ 3.220
R1234ze (E)	Cousins and Laesecke (2012) [170]	20 ^{satl}	247 ÷ 340	0.072 ÷ 1.499
	Grebenkov et al. (2009) [43]	35 ^{cl} + 18 ^{sv}	257 ÷ 369	0.990 ÷ 6.080
	Meng et al. (2013) [173]	119 ^{cl}	243 ÷ 373	Saturation ÷ 30.000
	Zhao et al. (2014) [175]	9 ^{satl}	295 ÷ 373	At saturation
R1336mzz(E)	Mondal et al. (2022) [176]	38 ^{cl} + 36 ^{sv} + 18 ^{scr}	413 ÷ 453	3.000 ÷ 4.000
	Xu et al. (2021) [177]	10 ^{cl}	278 ÷ 333	At saturation
	Zhang et al. (2022) [169]	22 ^{sat l}	303 ÷ 442	At saturation
R1234ze(Z)	Kariya et al. (2015) ^a [178]	(N.A.) ^{cl+sv}	283 ÷ 363	0.180 ÷ 1.350
	Kariya et al. (2017) ^a [179]	N.A.	290 ÷ 440	0.500 ÷ 3.000
	Alam et al. (2021) [180]	59 ^{cl} + 31 ^{sv}	314 ÷ 414	0.500 ÷ 4.800
R1224yd(Z)	Miyara et al. (2018) [167]	20 ^{cl} + 12 ^{sv}	303 ÷ 475	1.960 ÷ 3.210
	Alam et al. (2019) [162]	68 ^{cl} + 36 ^{sv}	303 ÷ 475	1.000 ÷ 4.100
R1233zd(E)	Hulse et al. (2012) [50]	6 ^{cl}	270 ÷ 380	0.100 ÷ 1.350
	Cui et al. (2018) [165]	12 ^{sat l}	303 ÷ 403	-
	Meng et al. (2018) [166]	92 ^{cl}	243 ÷ 373	< 40.000
	Miyara et al. (2018) [167]	61 ^{cl} + 28 ^{sv}	314 ÷ 474	1.010 ÷ 4.070
	Zhao et al. (2021) [163]	14 ^{sat l}	303 ÷ 432	0.150 ÷ 3.220
R1336mzz(Z)	Alam et al. (2018) [168]	71 ^{cl} + 26 ^{sv}	314 ÷ 475	0.490 ÷ 4.060
	Sun et al. (2019) [97]	109 ^{cl}	253 ÷ 353	< 40.000
	Zhang et al. (2022) [169]	20 ^{sat l}	303 ÷ 399	At saturation

^{cl}Compressed liquid^{sv}Superheated vapor^{scr}Supercritical conditions^{sat l}Saturated liquid

(2018) [164] reported 20 data in the compressed liquid region and 12 in the superheated vapor region, while Alam et al. (2019) [162] presented 68 data in the compressed liquid region and 36 data in the superheated vapor region; for both the datasets some data points have been excluded (3 and 9 respectively) because they exceed the range of applicability of the correlation implemented in

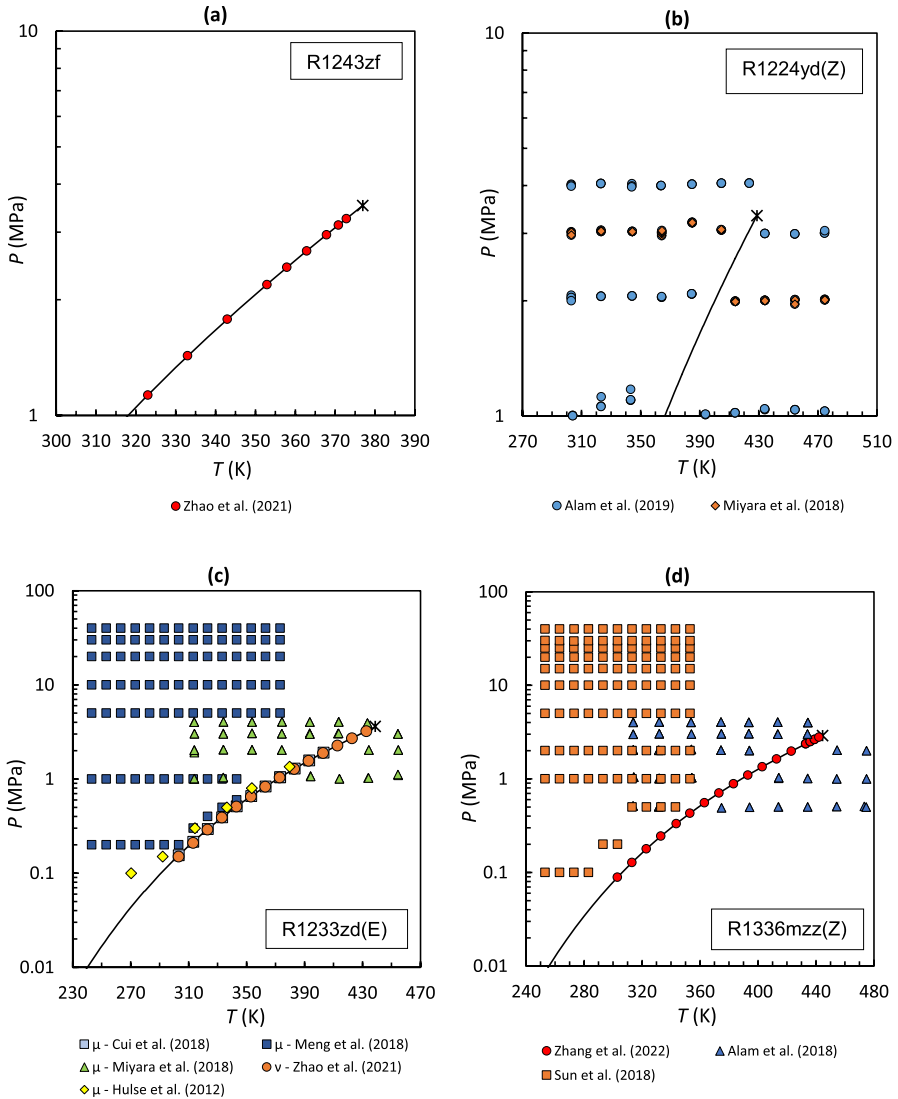


Fig. 12 Distribution on the P–T plane of the available viscosity data for (a) R1243zf, (b) R1224yd(Z), (c) R1233zd(E) and (d) R1336mzz(Z). Solid line: pressure curve. x: critical point

REFPROP. However, they seem in agreement with each other, both showing deviations below 4.2%.

R1233zd(E): a total of 5 data sets and 213 viscosity data is available today: 3 papers contain data in the compressed liquid region, 1 contains data in the superheated vapor region and 2 contain saturated liquid data. Among the data sets published after the review by Bobbo et al. (2018) [4], Cui et al. (2018) [165] reported 12 saturated liquid viscosities with AAD%=4.52 and MAD%=10.97, while other 14

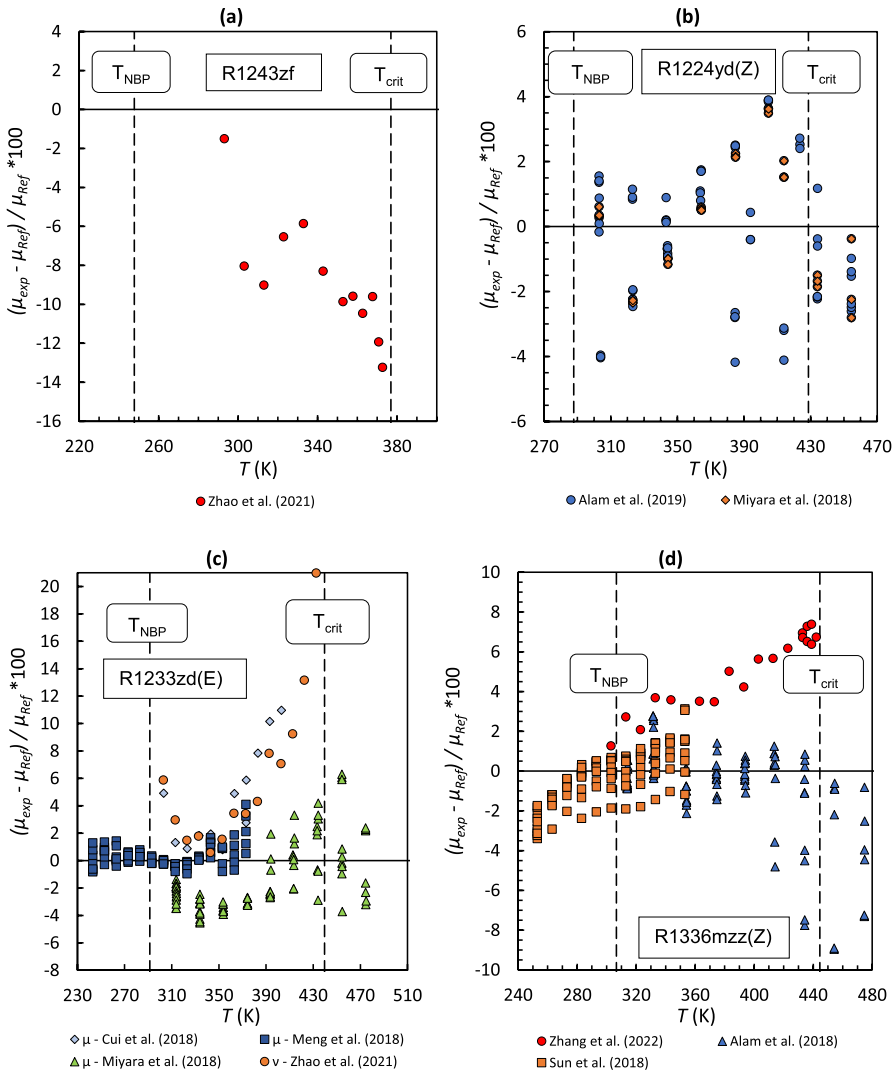


Fig. 13 Deviations of the experimental viscosity data for (a) R1243zf, (b) R1224yd(Z), (c) R1233zd(E) and (d) R1336mzz(Z) from the values calculated using REFPROP 10.0

data in saturated liquid conditions were provided by Zhao et al. (2021) [163] with AAD%=5.98 and MAD%=20.97, but in this case for kinematic viscosity. Meng et al. (2018) [166] and Miyara et al. (2018) [167] both reported compressed liquid viscosities showing two quite different deviations (AAD%=0.59 and AAD%=2.70 respectively). Moreover, Miyara et al. (2018) [167] also provided 28 data in the superheated vapor region, with AAD%=2.34 and MAD%=6.31.

R1336mzz(Z): since 2018 a total of 3 data sets (219 data) have been published in the peer-reviewed literature, two of them including data in the compressed liquid

Table 12 Available experimental data for the thermal surface tension of selected refrigerants

ASHRAE designation	References	No. data	T range (K)
R1123	Kano et al. (2020) [121]	16	267 ÷ 304
	Liu et al. (2021) [99]	28	232 ÷ 303
R1234yf	Tanaka and Higashi (2010a) [36]	29	273 ÷ 338
	Zhao et al. (2014) [175]	10	293 ÷ 365
	Liu et al. (2021) [99]	33	226 ÷ 343
R1243zf	Kondou et al. (2015) [183]	11	273 ÷ 352
	Zhao et al. (2021) [163]	12	303 ÷ 432
R1311	Duan et al. (1999) [184]	30	243 ÷ 344
R1234ze (E)	Grebekov et al. (2009) [43]	4	253 ÷ 313
	Tanaka and Higashi (2013) [185]	23	273 ÷ 333
	Zhao et al. (2014) [175]	9	295 ÷ 373
R1336mzz(E)	Zhang et al. (2022) [169]	22	303 ÷ 442
R1234ze(Z)	Kondou et al. (2015) [183]	13	273 ÷ 350
R1224yd(Z)	Kondou and Higashi (2018) [181]	19	266 ÷ 372
	Kondou et al. (2019) [182]	26	266 ÷ 372
R1233zd(E)	Hulse et al. (2012) [50]	3	273 ÷ 323
	Kondou et al. (2015) [183]	10	279 ÷ 350
	Cui et al. (2018) [165]	12	303 ÷ 403
	Zhao et al. (2021) [163]	14	303 ÷ 432
R1336mzz(Z)	Zhang et al. (2022) [169]	20	303 ÷ 399
R1130(E)	Tanaka et al. (2022) [13]	38	228 ÷ 373

region, one including data in the superheated vapor region and one for the saturated liquid. Sun et al. (2018) reported 109 data in the compressed liquid region showing good agreement with the equation of state from REFPROP in the range of temperatures 253 ÷ 353 K and for pressures lower than 40 MPa, with a final absolute average deviation $AAD\% = 1.075$. Deviations from Sun et al. (2019) [97] are in line with those obtained by Alam et al. (2018) [168] for the compressed liquid ($AAD\% = 0.78$), while data in the superheated vapor showed much higher deviations, with $AAD\% = 4.42$ and $MAD\% = 28.56$ (not shown in Fig. 13c). Finally, Zhang et al. (2022) [169] provided 20 saturated liquid viscosities in the range 303 K–399 K, with systematic positive deviations up to 7.38%.

2.3.3 Surface Tension

Compared to 2018, the number of fluids whose saturated liquid surface tension has been studied has more than doubled, from five in Bobbo et al. (2018) [4] to eleven at the present time. The publicly available datasets are listed in Table 12, along with their respective temperature range. R1233zd(E) has the highest number of available datasets, with four publications and 39 measurements in the range from 273 K to

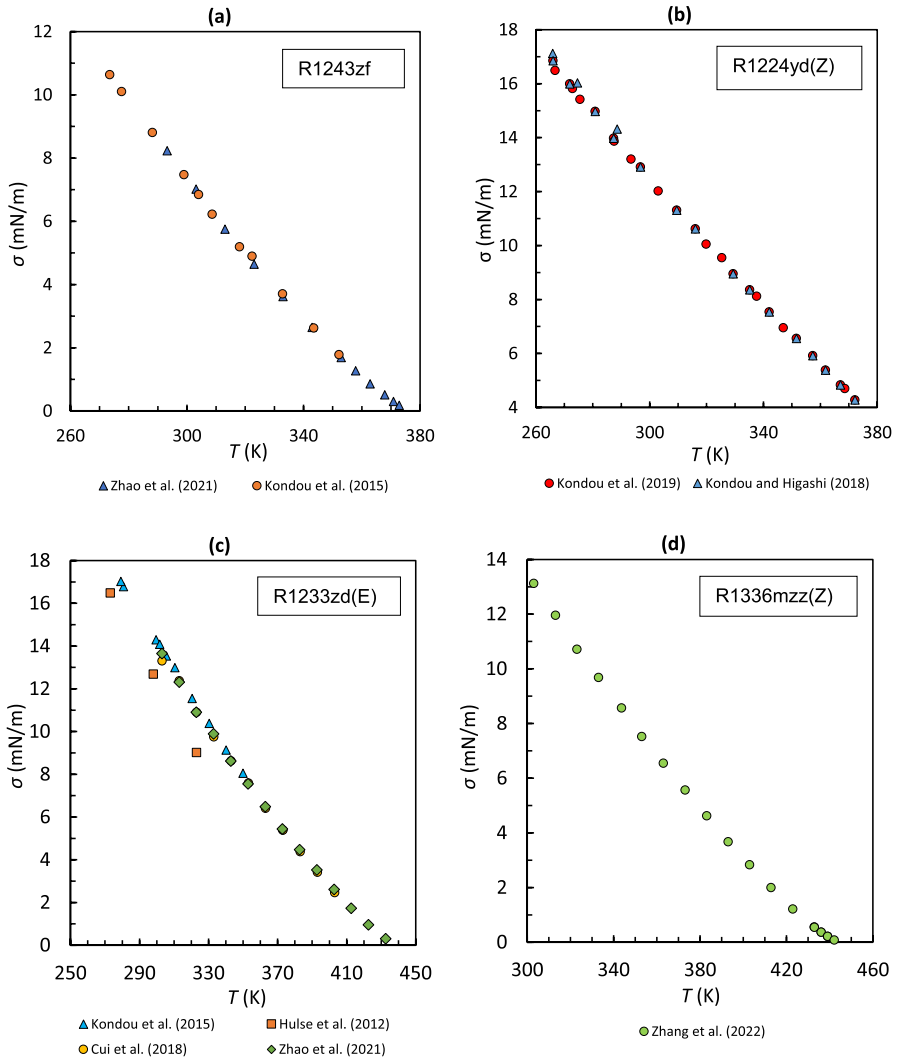


Fig. 14 Distribution on the σ – T plane of the available thermal surface tension data for (a) R1243zf, (b) R1224yd(Z), (c) R1233zd(E) and (d) R1336mzz(Z)

432 K, while R1336mzz(Z) is the least studied working fluid, with only one dataset and 20 data in the range from 303 K to 399 K. For R1243zf, compared to the review by Bobbo et al. (2018) [4], 12 additional data were measured in the range of 303 K to 432 K by Zhao et al. (2021) [163], while two different data sets were reported for R1224yd(Z) (Kondou and Higashi (2018) [181], Kondou (2019) [182]), totalling 35 data, both in the temperature range between 266 K and 372 K. The experimental data for the fluids are graphically displayed in Fig. 14.

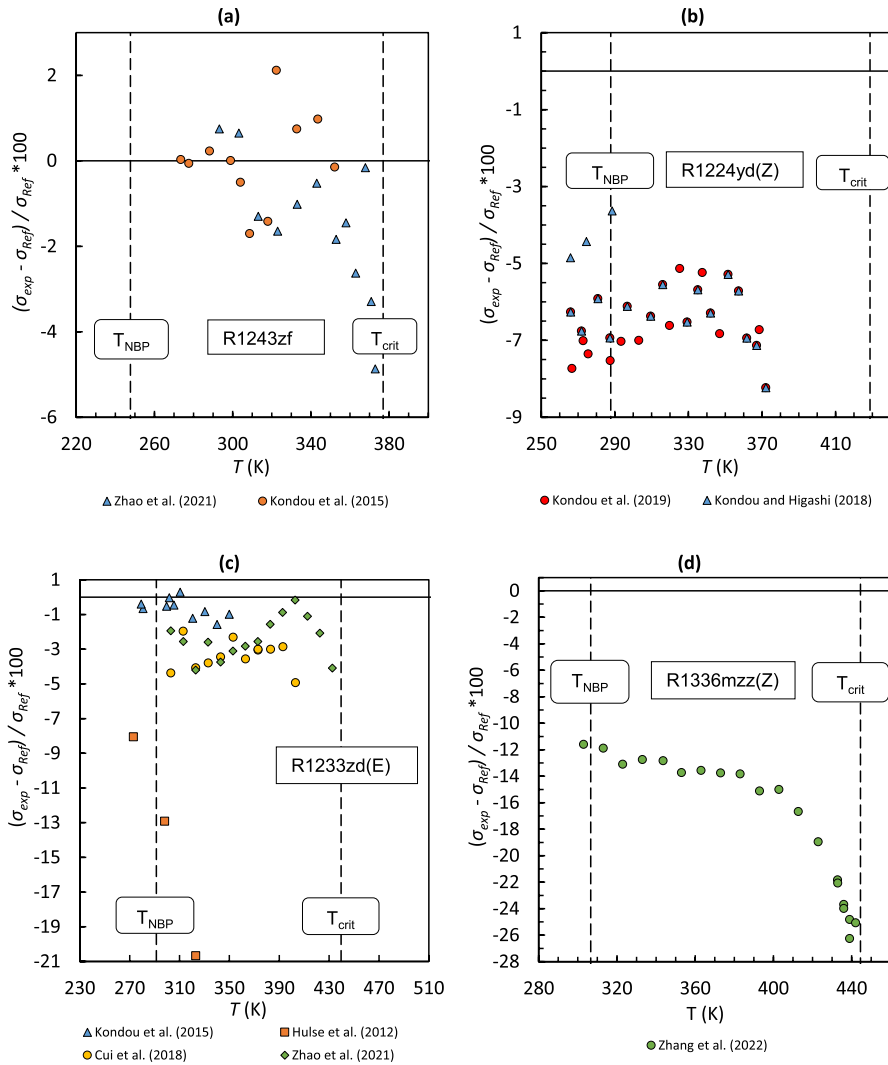


Fig. 15 Deviations of the experimental surface tension data for (a) R1243zf, (b) R1224yd(Z), (c) R1233zd(E) and (d) R1336mzz(Z) from the values calculated using REFPROP 10.0

The deviations from REFPROP 10.0 are shown in Fig. 15. To calculate the reference values for R1243zf and R1233zd(E), the empirical correlation presented by KlghfkljKondou et al. (2015) [183] and implemented in REFPROP was used. For R1224yd(Z) and R1336mzz(Z), on the other hand, no data were correlated at the time the latest version of the software was developed, so the values for these fluids were calculated using an ECS in predictive mode, with an estimated uncertainty of 10% [152].

3 Conclusions

It is a fact that for several HVAC&R applications there is still no definitive operating fluid able to simultaneously fulfil the requirements given by thermodynamic and new regulations addressing the Global Warming issue. As things stand today, the problem is often related to the lack of data on the thermophysical properties of new fluids. To this end, a literature search was conducted to identify new experimental data sets on the thermophysical properties of low global warming potential refrigerants published in the open literature during 2018 to 2022 and to update a previous review published in 2018. The amount of experimental data available for pure compounds, including refrigerants not considered in the previous review, has increased significantly in recent years, but research efforts are still needed to provide a complete description of all fluids of interest and to find the right substitutes for different applications. Currently, only 4 fluids have been fully investigated (R1234yf, R1234ze(E), R1233zd(E), R1243zf), while other 4 (R1234ze(Z), R1336mzz(Z), R1224yd(Z), R1336mzz(E)) have been almost completely characterised. For all fluids, several sets and a large amount of data are available for p_{sat} and PVT , while fewer sets are available for specific heat capacity and speed of sound. Especially for the transport properties, more information is needed. It must also be stressed that when searching for new refrigerants, it is not only thermodynamic properties that need to be considered, but also ODP, GWP, flammability, toxicity, and material compatibility; in particular, further clarifications are needed regards the possible environmental pollution created by HFOs.

Author Contributions GL, IG and DM collected the literature data, L.F and SG revised the data. All the authors reviewed the manuscript.

Funding Open access funding provided by Consiglio Nazionale Delle Ricerche (CNR) within the CRUI-CARE Agreement.

Data Availability Not applicable.

Declarations

Competing Interests The authors have no competing interests, or other interests that might be perceived to influence the results and/or discussion reported in this paper.

Ethical Approval Not applicable.

Open Access This article is licensed under a Creative Commons Attribution 4.0 International License, which permits use, sharing, adaptation, distribution and reproduction in any medium or format, as long as you give appropriate credit to the original author(s) and the source, provide a link to the Creative Commons licence, and indicate if changes were made. The images or other third party material in this article are included in the article's Creative Commons licence, unless indicated otherwise in a credit line to the material. If material is not included in the article's Creative Commons licence and your intended use is not permitted by statutory regulation or exceeds the permitted use, you will need to obtain permission directly from the copyright holder. To view a copy of this licence, visit <http://creativecommons.org/licenses/by/4.0/>.

References

1. J.M. Calm, *Int. J. Refrig.* **31**, 1123–1133 (2008). <https://doi.org/10.1016/j.ijrefrig.2008.01.013>
2. European Parliament and Council of the European Union, Regulation (EU) No 517/2014 of the European Parliament and of the Council of 16 April 2014 on fluorinated greenhouse gases and repealing Regulation (EC) No 842/2006 Text with EEA relevance. <http://data.europa.eu/eli/reg/2014/517/oj>. Accessed 10 Feb 2023.
3. M.O. McLinden, A.F. Kazakov, J. Steven Brown, P.A. Domanski, *Int. J. Refrig.* **38**, 80–92 (2014). <https://doi.org/10.1016/j.ijrefrig.2013.09.032>
4. S. Bobbo, G. Di Nicola, C. Zilio, J.S. Brown, L. Fedele, *Int. J. Refrig.* **90**, 181–201 (2018). <https://doi.org/10.1016/j.ijrefrig.2018.03.027>
5. E.W. Lemmon, I.H. Bell, M.L. Huber, M.O. McLinden, NIST Standard Reference Database 23: Reference Fluid Thermodynamic and Transport Properties-REFPROP, Version 10.0. National Institute of Standards and Technology (2018). <https://doi.org/10.18434/T4/1502528>.
6. M. O. McLinden, J. S. Brown, A. F. Kazakov, P. A. Domanski, et al., in *Proceedings of the 24th IIR International Congress of Refrigeration, Paper: keynote B1-We-1a* (2015). <https://doi.org/10.18462/iir.2015.1003>.
7. P. Giménez-Prades, J. Navarro-Esbri, C. Arpagaus, A. Fernández-Moreno, A. Mota-Babiloni, *Renew. Sustain. Energy Rev.* **167**, 112549 (2022). <https://doi.org/10.1016/j.rser.2022.112549>
8. G. Myhre, D. Shindell, J. Pongratz, in *Climate Change 2013: The Physical Science Basis. Contribution of Working Group I to the Fifth Assessment Report of the Intergovernmental Panel on Climate Change*, ed. by T.F. Stocker, D. Qin, G.-K. Plattner, M. Tignor, S.K. Allen, J. Boschung, A. Nauels, Y. Xia, V. Bex, P.M. Midgley (Cambridge University Press, Cambridge, 2014), p. 659
9. K. Tanaka, J. Ishikawa, K.K. Kontomaris, *Int. J. Refrig.* **33**, 474–479 (2017)
10. S. Tomassetti, G. Di Nicola, *Fluid Phase Equilib.* **533**, 112939 (2021). <https://doi.org/10.1016/j.fluid.2021.112939>
11. J.S. Brown, C. Zilio, A. Cavallini, *Int. J. Refrig.* **33**, 235–241 (2010). <https://doi.org/10.1016/j.ijrefrig.2009.04.005>
12. M.J. Alam, K. Kariya, K. Yamaguchi, Y. Hori, A. Miyara, *Int. J. Refrig.* **103**, 1–8 (2019). <https://doi.org/10.1016/j.ijrefrig.2019.03.024>
13. K. Tanaka, C. Kondou, S. Fukuda, R. Akasaka, *Int. J. Thermophys.* **43**, 69 (2022). <https://doi.org/10.1007/s10765-022-02986-2>
14. L. Fedele, G. Di Nicola, J.S. Brown, L. Colla, S. Bobbo, *Int. J. Refrig.* **69**, 243–250 (2016). <https://doi.org/10.1016/j.ijrefrig.2015.10.012>
15. R. Low, in *Proceedings of the 1st IIR International Conference on the Application of HFO Refrigerants*, Paper 1183 (2018). <https://doi.org/10.18462/iir.hfo.2018.1183>
16. R. Akasaka, M. Fukushima, E.W. Lemmon, in *International Refrigeration and Air Conditioning Conference*, Paper 1698 (2016). <http://docs.lib.purdue.edu/iracc/1698>. Accessed 10 Feb 2023
17. R. Akasaka, Y. Higashi, N. Sakoda, S. Fukuda, E.W. Lemmon, *Int. J. Refrig.* **119**, 457–467 (2020). <https://doi.org/10.1016/j.ijrefrig.2020.07.011>
18. R. Akasaka, *Int. J. Thermophys.* **32**, 1125–1147 (2011). <https://doi.org/10.1007/s10765-011-0992-0>
19. M. Richter, M.O. McLinden, E.W. Lemmon, *J. Chem. Eng. Data* **56**, 3254–3264 (2011). <https://doi.org/10.1021/jc200369m>
20. V. Rykov, A. Sverdllov, *J. Phys. Conf. Ser.* **1385**, 12013 (2019). <https://doi.org/10.1088/1742-6596/1385/1/012013>
21. E.W. Lemmon, R. Akasaka, *Int. J. Thermophys.* **43**, 119 (2022). <https://doi.org/10.1007/s10765-022-03015-y>
22. R. Akasaka, *Sci. Technol. Built Environ.* **22**, 1136–1144 (2016). <https://doi.org/10.1080/23744731.2016.1208000>
23. R. Akasaka, E.W. Lemmon, *J. Chem. Eng. Data* **64**, 4679–4691 (2019). <https://doi.org/10.1021/acs.jced.9b00007>
24. E.W. Lemmon, R. Span, *J. Chem. Eng. Data* **60**, 3745–3758 (2015). <https://doi.org/10.1021/acs.jced.5b00684>
25. M. Thol, E.W. Lemmon, *Int. J. Thermophys.* **37**, 1–16 (2016)
26. I.M. Astina, G. Budiarsa, R. Harrison, *Fluid Phase Equilib.* **531**, 112921–23 (2021). <https://doi.org/10.1016/j.fluid.2020.112921>

27. R. Akasaka, L.D. Simoni, E.W. Lemmon, in *International Refrigeration and Air Conditioning Conference*, Paper 2314 (2022). <https://docs.lib.purdue.edu/iracc/2314>. Accessed 10 Feb 2023
28. R. Akasaka, Y. Higashi, A. Miyara, S. Koyama, *Int. J. Refrig.* **44**, 168–176 (2014). <https://doi.org/10.1016/j.ijrefrig.2013.12.018>
29. R. Akasaka, M. Fukushima, and E. W. Lemmon, in *Proceedings of the 21st European Conference on Thermophysical Properties*, Paper 192 (2017)
30. M.E. Mondéjar, M.O. McLinden, E.W. Lemmon, *J. Chem. Eng. Data* **60**, 2477–2489 (2015). <https://doi.org/10.1021/acs.jced.5b00348>
31. R. Akasaka, E.W. Lemmon, *J. Phys. Chem. Ref. Data* **51**, 023101 (2022). <https://doi.org/10.1063/5.0083026>
32. M.O. McLinden, R. Akasaka, *J. Chem. Eng. Data* **65**, 4201–4214 (2020). <https://doi.org/10.1021/acs.jced.9b01198>
33. M. Fukushima, H. Hayamizu, M. Hashimoto, in *Proceedings of the 24th IIR International Congress of Refrigeration*, Paper 443 (2015)
34. Y. Higashi, R. Akasaka, in *Proceedings of the 16th International Refrigeration and Air Conditioning Conference*, Paper 1688 (2016). <http://docs.lib.purdue.edu/iracc/1688>. Accessed 10 Feb 2023
35. N. Sakoda, U.A. Perera, K. Thu, Y. Higashi, *Int. J. Refrig.* **140**, 166–171 (2022). <https://doi.org/10.1016/j.ijrefrig.2022.05.012>
36. K. Tanaka, Y. Higashi, *Int. J. Refrig.* **33**, 474–479 (2010). <https://doi.org/10.1016/j.ijrefrig.2009.10.003>
37. R. Hulse, R. Singh, H. Pham, in *Proceedings of the 3rd Conference on Thermophysical Properties and Transfer Processes of Refrigerants*, Paper 178 (2009). <https://iifir.org/en/fridoc/physical-properties-of-hfo-1234yf-26354>. Accessed 10 Feb 2023
38. T.E. Daubert, J.W. Jalowka, V. Goren, *AIChE Symp. Ser.* **83**, 128–156 (1987)
39. Y. Higashi, N. Sakoda, *J. Chem. Eng. Data* **63**, 3818–3822 (2018). <https://doi.org/10.1021/acs.jced.8b00452>
40. Y.Y. Duan, L. Shi, M.S. Zhu, L.Z. Han, *J. Chem. Eng. Data* **44**, 501–504 (1999). <https://doi.org/10.1021/je980251b>
41. U.A. Perera, K. Thu, N. Sakoda, M. Kozue, Y. Higashi, *J. Chem. Eng. Data* **67**, 2182–2192 (2022). <https://doi.org/10.1021/acs.jced.2c00182>
42. Y. Higashi, K. Tanaka, T. Ichikawa, *J. Chem. Eng. Data* **55**, 1594–1597 (2010). <https://doi.org/10.1021/je900696z>
43. A.J. Grebenkov, R. Hulse, H. Pham, R. Singh, in *Proceedings of the 3rd IIR Conference on Thermophysical Properties and Transfer Processes of Refrigerants*, Paper 191 (2009)
44. N. Sakoda, Y. Higashi, R. Akasaka, *J. Chem. Eng. Data* **66**, 734–739 (2021). <https://doi.org/10.1021/acs.jced.0c00848>
45. Y. Higashi, S. Hayasaka, C. Shirai, R. Akasaka, *Int. J. Refrig.* **52**, 100–108 (2015). <https://doi.org/10.1016/j.ijrefrig.2014.12.007>
46. K. Tanaka, *Trans. Jpn. Soc. Refrig. Air Condit. Eng.* **37**, 67–68 (2020). https://doi.org/10.1132/tjsrae.19-35TG_EM
47. N. Sakoda, Y. Higashi, *J. Chem. Eng. Data* **64**, 3983–3987 (2019). <https://doi.org/10.1021/acs.jced.9b00374>
48. K. Tanaka, R. Akasaka, *Int. J. Refrig.* **131**, 61–67 (2021). <https://doi.org/10.1016/j.ijrefrig.2021.07.010>
49. T. Kimura, Y. Kayukawa, H. Miyamoto, K. Saito, *Int. J. Thermophys.* **38**, 8 (2017). <https://doi.org/10.1007/s10765-017-2256-0>
50. R.J. Hulse, R.S. Basu, R.R. Singh, R.H.P. Thomas, *J. Chem. Eng. Data* **57**, 3581–3586 (2012). <https://doi.org/10.1021/je300776s>
51. K. Tanaka, R. Akasaka, E. Sakaue, J. Ishikawa, K.K. Kontomaris, *J. Chem. Eng. Data* **62**, 1135–1138 (2017). <https://doi.org/10.1021/acs.jced.6b00990>
52. T. Sako, M. Yasumoto, M. Sato, O. Kitao, K. Ishiguro, M. Kato, *Fluid Phase Equilib.* **144**, 113–117 (1998). [https://doi.org/10.1016/S0378-3812\(97\)00249-5](https://doi.org/10.1016/S0378-3812(97)00249-5)
53. Z. Yang, X. Tang, J. Wu, J. Lu, *Fluid Phase Equilib.* **498**, 86–93 (2019). <https://doi.org/10.1016/j.fluid.2019.06.020>
54. J. Yin, J. Ke, G. Zhao, S. Ma, *Int. J. Refrig.* **117**, 175–180 (2020). <https://doi.org/10.1016/j.ijrefrig.2020.04.021>
55. S. Bobbo, A. Bet, M. Scattolini, L. Fedele, *J. Chem. Eng. Data* **65**, 4263–4267 (2020). <https://doi.org/10.1021/acs.jced.0c00231>

56. G. Beltramino, L. Rosso, R. Cuccaro, V. Fericola, *Int. J. Refrig.* **145**, 90–95 (2023). <https://doi.org/10.1016/j.ijrefrig.2022.09.026>
57. S. Li, F. Yang, K. Zhang, Y. Duan, Z. Yang, *J. Chem. Eng. Data* **64**, 2947–2954 (2019). <https://doi.org/10.1021/acs.jced.9b00001>
58. N. Sakoda, Y. Higashi, R. Akasaka, *J. Chem. Eng. Data* **65**, 4285–4289 (2020). <https://doi.org/10.1021/acs.jced.0c00239>
59. J. Yin, J. Ke, G. Zhao, S. Ma, *Int. J. Refrig.* **121**, 253–257 (2021). <https://doi.org/10.1016/j.ijrefrig.2020.09.010>
60. S. Li, L. Xu, H. Liu, Z. Yang, Y. Duan, *J. Chem. Eng. Data* **65**, 4223–4229 (2020). <https://doi.org/10.1021/acs.jced.0c00024>
61. Y. Higashi, N. Sakoda, M.A. Islam, Y. Takata, S. Koyama, R. Akasaka, *J. Chem. Eng. Data* **63**, 417–421 (2018). <https://doi.org/10.1021/acs.jced.7b00818>
62. U.A. Perera, N. Sakoda, T. Miyazaki, K. Thu, Y. Higashi, *Int. J. Refrig.* **135**, 148–153 (2022). <https://doi.org/10.1016/j.ijrefrig.2021.12.014>
63. L.-X. Chen, P. Hu, W.-B. Zhu, L. Jia, Z.-S. Chen, *Fluid Phase Equilib.* **392**, 19–23 (2015). <https://doi.org/10.1016/j.fluid.2015.02.014>
64. G. Di Nicola, F. Polonara, G. Santori, *J. Chem. Eng. Data* **55**, 201–204 (2010). <https://doi.org/10.1021/je900306v>
65. L. Fedele, S. Bobbo, F. Groppo, J.S. Brown, C. Zilio, *J. Chem. Eng. Data* **56**, 2608–2612 (2011). <https://doi.org/10.1021/jc2000952>
66. P. Hu, X.-D. Cai, L.-X. Chen, H. Xu, G. Zhao, *J. Chem. Eng. Data* **62**, 3353–3359 (2017). <https://doi.org/10.1021/acs.jced.7b00427>
67. T. Kamiaka, C. Dang, E. Hihara, *Int. J. Refrig.* **36**, 965–971 (2013). <https://doi.org/10.1016/j.ijrefrig.2012.08.016>
68. T.M. Kochenburger, D. Gomse, I. Tratschitt, A. Zimmermann, S. Grohmann, *Fluid Phase Equilib.* **450**, 13–23 (2017). <https://doi.org/10.1016/j.fluid.2017.07.002>
69. H. Madani et al., *Fluid Phase Equilib.* **415**, 158–165 (2016). <https://doi.org/10.1016/j.fluid.2016.02.005>
70. Z. Yang et al., *Fluid Phase Equilib.* **427**, 390–393 (2016). <https://doi.org/10.1016/j.fluid.2016.07.031>
71. J. Yin, G. Zhao, S. Ma, *Int. J. Refrig.* **107**, 183–190 (2019). <https://doi.org/10.1016/j.ijrefrig.2019.08.008>
72. J. Brown, G. Nicola, L. Fedele, S. Bobbo, C. Zilio, *Fluid Phase Equilib.* **351**, 48–52 (2013). <https://doi.org/10.1016/j.fluid.2012.09.036>
73. Y.-Y. Duan, M.-S. Zhu, L.-Z. Han, *Fluid Phase Equilib.* **121**, 227–234 (1996). [https://doi.org/10.1016/0378-3812\(96\)03005-1](https://doi.org/10.1016/0378-3812(96)03005-1)
74. G. Di Nicola, J.S. Brown, L. Fedele, S. Bobbo, C. Zilio, *J. Chem. Eng. Data* **57**, 2197–2202 (2012). <https://doi.org/10.1021/jc300240k>
75. X. Dong, M. Gong, J. Shen, J. Wu, *Int. J. Refrig.* **34**, 1238–1243 (2011). <https://doi.org/10.1016/j.ijrefrig.2011.03.007>
76. X. Dong, M. Gong, J. Shen, J. Wu, *J. Chem. Eng. Data* **57**, 541–544 (2012). <https://doi.org/10.1021/jc2011055>
77. X. Dong, H. Guo, M. Gong, Z. Yang, J. Wu, *J. Chem. Thermodyn.* **60**, 25–28 (2013). <https://doi.org/10.1016/j.jct.2012.12.026>
78. M. Gong et al., *Int. J. Refrig.* **64**, 168–175 (2016). <https://doi.org/10.1016/j.ijrefrig.2016.01.007>
79. X. Hu, X. Meng, J. Wu, *Fluid Phase Equilib.* **431**, 58–65 (2017). <https://doi.org/10.1016/j.fluid.2016.10.011>
80. Y. Kayukawa, K. Fujii, in *Proceedings of the 2009 Symposium on the Environmental Engineering*, Paper A134 (2009)
81. M.O. McLinden, M. Thol, E.W. Lemmon, in *Proceedings of the International Refrigeration and Air Conditioning Conference*, Paper 1041 (2010). <http://docs.lib.purdue.edu/iracc/1041>. Accessed 10 Feb 2023
82. T. Katsuyuki, *J. Chem. Eng. Data* **61**, 1645–1648 (2016). <https://doi.org/10.1021/acs.jced.5b01039>
83. K. Tanaka, G. Takahashi, Y. Higashi, *J. Chem. Eng. Data* **55**, 2169–2172 (2010). <https://doi.org/10.1021/jc900756g>
84. J. Yin, Y. Zhou, G. Zhao, S. Ma, *Fluid Phase Equilib.* **460**, 69–74 (2018). <https://doi.org/10.1016/j.fluid.2017.12.030>

85. L. Fedele, G. Di Nicola, J.S. Brown, S. Bobbo, C. Zilio, *Int. J. Thermophys.* **35**, 1–12 (2014). <https://doi.org/10.1007/s10765-013-1553-5>
86. Y. Kayukawa, K. Tanaka, Y. Kano, Y. Fujita, R. Akasaka, Y. Higashi, Experimental evaluation of the fundamental properties of low-GWP refrigerant R-1234ze (Z), in *Proceedings of the International Symposium on New Refrigerants and Environmental Technology* (2012)
87. N. Sakoda, J. Shiheng, M. Kohno, S. Koyama, Y. Higashi, Y. Takata, *J. Chem. Eng. Data* **62**, 2178–2182 (2017). <https://doi.org/10.1021/acs.jced.7b00263>
88. K. Zhuo, Y. Zhao, X. Dong, M. Gong, J. Wu, *Kexue Tongbao/Chin. Sci. Bull.* **62**, 2691–2697 (2017). <https://doi.org/10.1360/N972016-00615>
89. X. Zhang, *J. Thermophys. Heat Transf.* **33**, 779–784 (2019). <https://doi.org/10.2514/1.T5513>
90. T. Kimura, Y. Kayukawa, K. Saito, *J. Chem. Eng. Data* **62**, 1422–1426 (2017). <https://doi.org/10.1021/acs.jced.6b00980>
91. G. Di Nicola, L. Fedele, J.S. Brown, S. Bobbo, G. Coccia, *J. Chem. Eng. Data* **62**, 2496–2500 (2017). <https://doi.org/10.1021/acs.jced.6b00916>
92. K. Tanaka, *Trans. JSRAE* **33**, 105–111 (2016). https://doi.org/10.11322/tjsrae.15-48_OA
93. V. Machat, T. Boublik, *J. Chem. Thermodyn.* **17**, 887–891 (1985). [https://doi.org/10.1016/0021-9614\(85\)90082-5](https://doi.org/10.1016/0021-9614(85)90082-5)
94. L. Fedele, S. Bobbo, M. Scattolini, C. Zilio, R. Akasaka, *Int. J. Refrig.* **118**, 139–145 (2020). <https://doi.org/10.1016/j.jrefrig.2020.06.001>
95. S. Lago, Data to be Published (2022)***
96. K. Tanaka, *J. Chem. Eng. Data* **61**, 3570–3572 (2016). <https://doi.org/10.1021/acs.jced.6b00502>
97. Y. Sun, X. Li, X. Meng, J. Wu, *J. Chem. Eng. Data* **64**, 395–403 (2019). <https://doi.org/10.1021/acs.jced.8b00713>
98. Y. Kayukawa, *Int. J. Refrig.* **119**, 349–355 (2020). <https://doi.org/10.1016/j.jrefrig.2020.07.010>
99. Y. Liu, C. Kondou, C. Coquelet, C. Houriez, *Int. J. Refrig.* **132**, 276–292 (2021). <https://doi.org/10.1016/j.jrefrig.2021.09.021>
100. L. Fedele, J.S. Brown, L. Colla, A. Ferron, S. Bobbo, C. Zilio, *J. Chem. Eng. Data* **57**, 482–489 (2012). <https://doi.org/10.1021/je201030g>
101. J. Klomfar, M. Součková, J. Pátek, *J. Chem. Eng. Data* **57**, 3283–3289 (2012). <https://doi.org/10.1021/je3009304>
102. G. Qiu, X. Meng, J. Wu, *J. Chem. Thermodyn.* **60**, 150–158 (2013). <https://doi.org/10.1016/j.jct.2013.01.006>
103. M. Yoshitake, S. Matsuo, T. Sotani, Density and speed of sound measurements of HFC-1234yf, in *Proceedings of the 30th Japan Symposium on Thermophysical Properties*, pp. 353–355 (2009)
104. C. Di Nicola, G. Di Nicola, M. Pacetti, F. Polonara, G. Santori, *J. Chem. Eng. Data* **55**, 3302–3306 (2010). <https://doi.org/10.1021/je100102q>
105. G. Di Nicola, J. StevenBrown, L. Fedele, M. Securo, S. Bobbo, C. Zilio, *Int. J. Refrig.* **36**, 2209–2215 (2013). <https://doi.org/10.1016/j.jrefrig.2013.08.004>
106. Y.-Y. Duan, M.-S. Zhu, L. Shi, L.-Z. Han, *Fluid Phase Equilib.* **131**, 233–241 (1997). [https://doi.org/10.1016/S0378-3812\(96\)03227-X](https://doi.org/10.1016/S0378-3812(96)03227-X)
107. J. Klomfar, M. Součková, J. Pátek, *J. Chem. Eng. Data* **57**, 3270–3277 (2012). <https://doi.org/10.1021/je3008974>
108. J.S. Brown, G. Di Nicola, C. Zilio, L. Fedele, S. Bobbo, F. Polonara, *J. Chem. Eng. Data* **57**, 3710–3720 (2012). <https://doi.org/10.1021/je300945r>
109. K. Yamaya, A. Matsuguchi, N. Kagawa, S. Koyama, *J. Chem. Eng. Data* **56**, 1535–1539 (2011). <https://doi.org/10.1021/je101209e>
110. K. Zhang, H. Chen, Z. Yang, Y. Duan, *J. Chem. Thermodyn.* **149**, 106160 (2020). <https://doi.org/10.1016/j.jct.2020.106160>
111. K. Tanaka, Y. Higashi, *J. Chem. Eng. Data* **55**, 5164–5168 (2010). <https://doi.org/10.1021/je100707s>
112. H. Zhang, M. Gong, H. Li, H. Guo, X. Dong, J. Wu, *Fluid Phase Equilib.* **408**, 232–239 (2016). <https://doi.org/10.1016/j.fluid.2015.09.010>
113. J.S. Brown, L. Fedele, G. Di Nicola, S. Bobbo, G. Coccia, *J. Chem. Eng. Data* **60**, 3333–3340 (2015). <https://doi.org/10.1021/acs.jced.5b00562>
114. K. Tanaka, J. Ishikawa, K.K. Kontomaris, *J. Chem. Eng. Data* **62**, 2450–2453 (2017). <https://doi.org/10.1021/acs.jced.7b00381>
115. R. Romeo, P.A. Giuliano Albo, S. Lago, J.S. Brown, *Int. J. Refrig.* **79**, 176–182 (2017). <https://doi.org/10.1016/j.jrefrig.2017.04.003>

116. K. Tanaka, K. Maruko, Y. Fujimoto, M. Tanaka, in *Proceedings of Fourth Conference on Thermophysical Properties and Transfer Processes of Refrigerants*, Paper 072 (2013)
117. Y. Kayukawa, T. Kimura, Y. Kano, Y. Fujita, K. Saito, Thermodynamic property measurements for hydrofluorobutenes by a magnetic levitation densimeter, in *Proceedings of the 24th IIR International Congress of Refrigeration (ICR2015)* (2015)
118. L. Fedele, M. Pierantozzi, G. Di Nicola, J.S. Brown, S. Bobbo, J. Chem. Eng. Data **63**, 225–232 (2018). <https://doi.org/10.1021/acs.jced.7b00841>
119. K. Tanaka, R. Akasaka, E. Sakaue, J. Ishikawa, K.K. Kontomaris, J. Chem. Eng. Data **61**, 2467–2473 (2016). <https://doi.org/10.1021/acs.jced.6b00169>
120. Q. Chen, R. Gao, X. Guan, L. Du, G. Chen, L. Tang, J. Chem. Eng. Data **65**, 4230–4235 (2020). <https://doi.org/10.1021/acs.jced.0c00219>
121. Y. Kano, *Energies* **13**, 5525 (2020). <https://doi.org/10.3390/en13205525>
122. Q. Chen et al., J. Chem. Eng. Data **65**, 4790–4797 (2020). <https://doi.org/10.1021/acs.jced.0c00232>
123. L. Ding et al., J. Chem. Thermodyn. **161**, 106494 (2021). <https://doi.org/10.1016/j.jct.2021.106494>
124. Y. Liu, X. Zhao, Int. J. Refrig. **86**, 127–132 (2018). <https://doi.org/10.1016/j.ijrefrig.2017.11.015>
125. N. Gao, Y. Jiang, J. Wu, Y. He, G. Chen, Fluid Phase Equilib. **376**, 64–68 (2014). <https://doi.org/10.1016/j.fluid.2014.05.029>
126. Y. Kano, Y. Kayukawa, K. Fujii, H. Sato, Int. J. Thermophys. **31**, 2051–2058 (2010). <https://doi.org/10.1007/s10765-010-0885-7>
127. Y. Liu, X. Zhao, S. Lv, H. He, J. Chem. Eng. Data **62**, 1119–1124 (2017). <https://doi.org/10.1021/acs.jced.6b00959>
128. K. Tanaka, G. Takahashi, Y. Higashi, J. Chem. Eng. Data **55**, 2267–2270 (2010). <https://doi.org/10.1021/je900799e>
129. N. Kagawa, A. Matsuguchi, J. Chem. Eng. Data **65**, 4299–4305 (2020). <https://doi.org/10.1021/acs.jced.0c00243>
130. M.Z. Lukawski, M.P.E. Ishmael, J.W. Tester, J. Chem. Eng. Data **63**, 463–469 (2018). <https://doi.org/10.1021/acs.jced.7b00946>
131. Q. Zhong et al., J. Chem. Thermodyn. **125**, 86–92 (2018). <https://doi.org/10.1016/j.jct.2018.05.022>
132. B. Sheng, Y. Zhao, X. Dong, H. Guo, M. Gong, J. Chem. Thermodyn. **164**, 106626 (2022). <https://doi.org/10.1016/j.jct.2021.106626>
133. B. Sheng et al., J. Chem. Thermodyn. **153**, 106319 (2021). <https://doi.org/10.1016/j.jct.2020.106319>
134. Y.Y. Duan, L.Q. Sun, L. Shi, M.S. Zhu, L.Z. Han, Fluid Phase Equilib. **137**, 121–131 (1997). [https://doi.org/10.1016/S0378-3812\(97\)00152-0](https://doi.org/10.1016/S0378-3812(97)00152-0)
135. N. Gao, G. Chen, R. Li, Y. Wang, Y. He, B. Yang, J. Therm. Anal. Calorim. **122**, 1469–1476 (2015). <https://doi.org/10.1007/s10973-015-4837-0>
136. N. Kagawa, A. Matsuguchi, K. Watanabe, Trans. JSRAE **28**, 71–76 (2011)
137. Y. Kano, Y. Kayukawa, K. Fujii, H. Sato, J. Chem. Eng. Data **58**, 2966–2969 (2013). <https://doi.org/10.1021/je4004564>
138. Y. Liu, X. Zhao, H. He, R. Wang, J. Chem. Eng. Data **63**, 113–118 (2018). <https://doi.org/10.1021/acs.jced.7b00713>
139. K. Yamaya, A. Matsuguchi, N. Kagawa, in *Proceedings of the 23rd IIR International Congress of Refrigeration*, Paper 303 (2011)
140. L. Wang et al., J. Chem. Thermodyn. **141**, 105936–38 (2020). <https://doi.org/10.1016/j.jct.2019.105936>
141. Y. Kano, Y. Kayukawa, Y. Fujita, Int. J. Refrig. **118**, 354–364 (2020). <https://doi.org/10.1016/j.ijrefrig.2020.06.027>
142. H. Chen, K. Zhang, Z. Yang, Y. Duan, J. Chem. Eng. Data **66**, 2256–2263 (2021). <https://doi.org/10.1021/acs.jced.1c00098>
143. S. Lago, P.A. Giuliano Albo, J.S. Brown, M. Bertinetti, J. Chem. Eng. Data **63**, 4039–4045 (2018). <https://doi.org/10.1021/acs.jced.8b00427>
144. Y. Kano, J. Chem. Thermodyn. **159**, 106448 (2021). <https://doi.org/10.1016/j.jct.2021.106448>
145. X. Peng, H. Liu, L. Xu, Z. Yang, Y. Duan, J. Chem. Thermodyn. **171**, 106808 (2022). <https://doi.org/10.1016/j.jct.2022.106808>
146. L. Gao, T. Shibusaki, T. Honda, H. Asou, Adv. Mater. Res. **875–877**, 588–592 (2014). <https://doi.org/10.4028/www.scientific.net/AMR.875-877.588>

147. S. Lago, P.A.G. Albo, S. Brignolo, J. Chem. Eng. Data **56**, 161–163 (2011). <https://doi.org/10.1021/je100896n>
148. M.O. McLinden, R.A. Perkins, A dual-path pulse-echo instrument for liquid-phase speed of sound and measurements on four halogenated-olefin refrigerants [HFO-1234yf, HFO-1234ze(E), HFCO-1233zd(E), and HFO-1336mzz(Z)]. Ind. Engr. Chem. Res. (2023), to be published
149. R.A. Perkins, M.O. McLinden, J. Chem. Thermodyn. **91**, 43–61 (2015). <https://doi.org/10.1016/j.jct.2015.07.005>
150. S. Lago, P.A. Giuliano Albo, J.S. Brown, Int. J. Refrig. **65**, 55–59 (2016). <https://doi.org/10.1016/j.jrefrig.2016.02.003>
151. D. Lozano-Martín, D.M. Ripa, R.M. Gavioso, Int. J. Refrig. **100**, 37–47 (2019). <https://doi.org/10.1016/j.jrefrig.2019.01.021>
152. M.L. Huber, Models for viscosity, thermal conductivity, and surface tension of selected pure fluids as implemented in REFPROP v10.0, in *NIST Interagency/Internal Report (NISTIR)* (National Institute of Standards and Technology, Gaithersburg, 2023). <https://doi.org/10.6028/NIST.IR.8209>. Accessed 10 Feb 2023
153. D. Kim et al., Int. J. Refrig. **131**, 990–999 (2021). <https://doi.org/10.1016/j.jrefrig.2021.07.019>
154. R.A. Perkins, M.L. Huber, M.J. Assael, J. Chem. Eng. Data **62**, 2659–2665 (2017). <https://doi.org/10.1021/acs.jced.7b00106>
155. M.J. Alam, M.A. Islam, K. Kariya, A. Miyara, Int. J. Refrig. **90**, 174–180 (2018). <https://doi.org/10.1016/j.jrefrig.2018.02.004>
156. M.J. Alam, M.A. Islam, K. Kariya, A. Miyara, Int. J. Refrig. **84**, 220–227 (2017). <https://doi.org/10.1016/j.jrefrig.2017.08.014>
157. R.A. Perkins, M.L. Huber, Int. J. Thermophys. **41**, 103 (2020). <https://doi.org/10.1007/s10765-020-02681-0>
158. R.A. Perkins, M.L. Huber, J. Chem. Eng. Data **56**, 4868–4874 (2011). <https://doi.org/10.1021/je200811n>
159. D. Mondal, K. Kariya, A.R. Tuhin, K. Miyoshi, A. Miyara, Int. J. Refrig. **129**, 109–117 (2021). <https://doi.org/10.1016/j.jrefrig.2021.05.005>
160. G. Haowen, W. Xilei, Z. Yuan, G. Zhikai, H. Xiaohong, C. Guangming, Ind. Eng. Chem. Res. **60**, 9592–9601 (2021). <https://doi.org/10.1021/acs.iecr.1c01228>
161. H. Ishida, S. Mori, K. Kariya, A. Miyara, Thermal conductivity measurements of low GWP refrigerants with hot-wire method, in *Proceedings of the 24th International Congress of Refrigeration (ICR)* (2015)
162. M.J. Alam, K. Yamaguchi, Y. Hori, K. Kariya, A. Miyara, Int. J. Refrig. **104**, 221–228 (2019). <https://doi.org/10.1016/j.jrefrig.2019.05.033>
163. G. Zhao, Z. Yuan, X. Zhang, J. Yin, S. Ma, Int. J. Refrig. **127**, 194–202 (2021). <https://doi.org/10.1016/j.jrefrig.2021.03.012>
164. A. Miyara, J. Alam, K. Kariya, in *Proceedings of the 1st IIR International Conference on the Application of HFO Refrigerants*, Paper 1139 (2018). <https://doi.org/10.18462/iir.hfo.2018.1139>
165. J. Cui, S. Yan, S. Bi, J. Wu, J. Chem. Eng. Data **63**, 751–756 (2018). <https://doi.org/10.1021/acs.jced.7b00902>
166. X. Meng, C. Wen, J. Wu, J. Chem. Thermodyn. **123**, 140–145 (2018). <https://doi.org/10.1016/j.jct.2018.04.001>
167. A. Miyara, M.J. Alam, K. Kariya, Int. J. Refrig. **92**, 86–93 (2018). <https://doi.org/10.1016/j.jrefrig.2018.05.021>
168. M.J. Alam, A. Miyara, K. Kariya, K.K. Kontomaris, J. Chem. Eng. Data **63**, 1706–1712 (2018). <https://doi.org/10.1021/acs.jced.8b00036>
169. X. Zhang, G. Zhao, J. Yin, S. Ma, Fluid Phase Equilib. **559**, 113468 (2022). <https://doi.org/10.1016/j.fluid.2022.113468>
170. D.S. Cousins, A. Laesecke, J. Res. Natl Inst. Stand. Technol. **117**, 231–256 (2012)
171. Y. Dang, T. Kamiaka, C. Dang, E. Hihara, J. Chem. Thermodyn. **89**, 183–188 (2015). <https://doi.org/10.1016/j.jct.2015.05.009>
172. Y. Dang, H.S. Kim, C. Dang, E. Hihara, Int. J. Refrig. **58**, 131–136 (2015). <https://doi.org/10.1016/j.jrefrig.2015.06.010>
173. X. Meng, G. Qiu, J. Wu, I.M. Abdulagatov, J. Chem. Thermodyn. **63**, 24–30 (2013). <https://doi.org/10.1016/j.jct.2013.03.013>

174. S. Yamaguchi, S. Matsuo, T. Sotani, Viscosity measurement of HFO1234yf by means of rolling-ball method, in *Proceedings of the 30th Japan Symposium on Thermophysical Properties*, pp. 350–352 (2010)
175. G. Zhao, S. Bi, A.P. Fröba, J. Wu, *J. Chem. Eng. Data* **59**, 1366–1371 (2014). <https://doi.org/10.1021/je5001457>
176. D. Mondal, K. Kariya, A.R. Tuhin, N. Amakusa, A. Miyara, *Int. J. Refrig.* **133**, 267–275 (2022). <https://doi.org/10.1016/j.ijrefrig.2021.10.006>
177. C. Xu et al., *J. Ciesc* **72**, 3261–3269 (2021). <https://doi.org/10.11949/0438-1157.20201597>
178. K. Kariya, S. Mori, A. Miyara, in *Proceedings of the 24th IIR International Congress of Refrigeration*, Paper 684 (2015). <https://doi.org/10.18462/iir.icr.2015.0684>
179. K. Kariya, M. A. Islam, A. M. Jahangir, H. Ishida, and A. Miyara, Transport properties measurement on low GWP alternative refrigerants, *AIP Conf. Proc.* **1788**, 20003 (2017). <https://doi.org/10.1063/1.4968251>
180. M.J. Alam, M.A. Islam, K. Kariya, A. Miyara, *Int. J. Refrig.* **131**, 341–347 (2021). <https://doi.org/10.1016/j.ijrefrig.2021.04.004>
181. C. Kondou, Y. Higashi, *Proceedings of the 1st IIR International Conference on the Application of HFO Refrigerants*, Paper 1126 (2018). <https://doi.org/10.18462/iir.hfo.2018.1126>
182. C. Kondou, Y. Higashi, S. Iwasaki, *J. Chem. Eng. Data* **64**, 5462–5468 (2019). <https://doi.org/10.1021/acs.jced.9b00613>
183. C. Kondou, R. Nagata, N. Nii, S. Koyama, Y. Higashi, *Int. J. Refrig.* **53**, 80–89 (2015). <https://doi.org/10.1016/j.ijrefrig.2015.01.005>
184. Y.-Y. Duan, L. Shi, M.-S. Zhu, L.-Z. Han, *Fluid Phase Equilib.* **154**, 71–77 (1999). [https://doi.org/10.1016/S0378-3812\(98\)00439-7](https://doi.org/10.1016/S0378-3812(98)00439-7)
185. K. Tanaka, Y. Higashi, *J. Chem. Eng. Jpn.* **46**, 371–375 (2013). <https://doi.org/10.1252/jcej.13we021>

Publisher's Note Springer Nature remains neutral with regard to jurisdictional claims in published maps and institutional affiliations.

Authors and Affiliations

L. Fedele¹ · G. Lombardo^{1,2} · I. Greselin³ · D. Menegazzo^{1,2} · S. Bobbo¹

¹ Construction Technologies Institute, National Research Council, Corso Stati Uniti 4, 35127 Padua, Italy

² Department of Industrial Engineering-Applied Physics Section, University of Padova, Via Venezia 1, 35131 Padua, Italy

³ Department of Management and Engineering, University of Padova, 36100 Vicenza, Italy